REPORT

Mary River Project

2021 and 2024 Ringed Seal Aerial Survey Program (RSASP) - Technical Report

Submitted to:

Baffinland Iron Mines Corporation

360 Oakville Place Drive - Suite 300, Oakville, Ontario, L6H 6K8

Submitted by:

WSP Canada Inc.

237 – 4th Avenue SW, Suite 3300, Calgary, Alberta, T2P 4K3, Canada

+1 403 299 5600

CA0051512.6683-001-R-Rev1

February 9, 2026

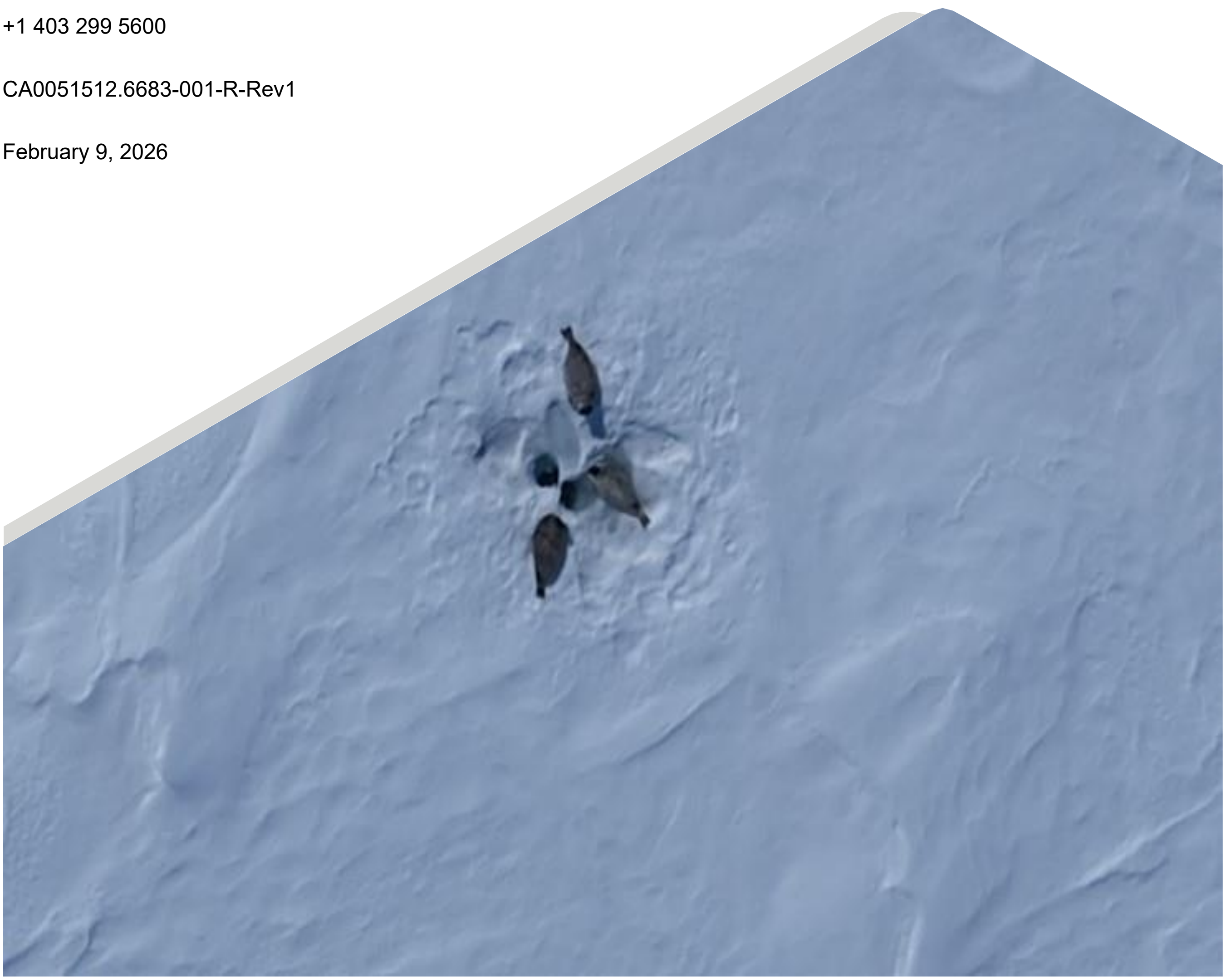

Distribution List

e-copy: Baffinland Iron Mines Corporation

e-copy: WSP Canada Inc.

ᐊᐅᓚᑦᑎᔾᓂᖒᖅᑐᑦ ᓇᐃᓈᖅᓯᒪᔪᖅ

ᓇᑦᑎᕐᓂᒃ ᖃᖓᑕᓲᒃᑯᑦ ᖃᐅᔨᓴᕐᓂᕐᒧᑦ ᐱᓕᕆᐊᖅ (RSASP) ᐱᓕᕆᐊᖑᓚᐅᖅᑐᑦ WSP-ᑯᓐᓂᑦ ᐊᒥᑦᑑᑉ ᐃᒪᖓᓂ (ᓯᑯᓰᓚᕐᒥ) ᓂᒋᐊᒍᑦ ᐅᒥᐊᕐᔪᐊᑦ ᐊᖅᑯᑎᒃᓴᖓᓂ ᔫᓂ 2021-ᒥ ᐊᒻᒪ 2024-ᒥ. ᑎᑭᑕᐅᓇᓱᒃᑐᐊᑕᖅᓯᒪᔪᖅ ᖃᐅᔨᓴᕐᑮᑎᓂᑦ ᓄᑖᙳᕆᐊᖅᑕᐅᕐᑯᒃᑐᒋᑦ ᐱᒋᐊᕈᑕᐅᔪᑦ ᖃᐅᔨᓴᕈᑏᑦ ᖃᐅᔨᓴᕈᑎᖏᑦ ᓇᑦᑏᑦ ᐱᑕᖃᐅᕐᓂᖏᑦ ᐊᒻᒪ ᓇᓃᖃᑦᑕᕐᓂᖏᑦ ᑐᕙᕐᒥ ᑕᐅᕚᓇ ᓂᒋᐊᒍᑦ ᐅᒥᐊᕐᔪᐊᑦ ᐊᖅᑯᑎᒃᓴᖓᓂ ᐃᒃᐱᑭᑦᑐᕐᔪᐊᓂ ᐊᒻᒪ ᖃᐅᔨᒋᐊᕐᕕᐅᔪᓐᓇᖅᑑᑉ ᓯᑯᖓᓂ (ᑕᓯᐅᔭᖅ). ᑭᖑᓪᓕᖅ ᑎᑭᑕᐅᓇᓱᐊᖅᑐᑦ ᖃᐅᔨᓴᕈᑎᓂ ᓇᓗᓇᐃᔭᖅᑕᐅᕐᑯᒃᑐᒋᑦ ᓇᑦᑏᑦ ᐱᑕᖃᐅᕐᕕᖏᑦ ᑐᕙᕐᒥ ᐃᒃᐱᑭᑦᑐᕐᔪᐊᓂ ᑕᓯᐅᔭᕐᒥᓗ.

ᒪᕐᕈᒃ ᐊᔾᔨᒌᙱᑐᒃ ᕿᒥᕐᕈᓃᑦ ᐱᓕᕆᐊᖑᓚᐅᖅᑑᒃ 2021-ᒥ ᐊᒻᒪ 2024-ᒥ ᖃᐅᔨᓴᕈᑎᕕᓂᕐᒍᑦ. ᑐᑭᓕᐊᖅᑐᓂᒃ ᕿᒥᕐᕈᓂᖅ ᐆᓇᕐᓃᑦ ᒪᓕᒃᑯᒋᑦ ᐊᔾᔨᙳᐊᑦ ᐱᖃᓯᐅᑎᓪᓗᒋᑦ ᖃᓇᓴᐅᔭᒃᑰᕈᓐᓇᖅᑐᑦ ᐊᔾᔨᙳᐊᑦ ᐊᑐᖅᑕᐅᓚᐅᖅᑐᑦ ᓈᓴᐅᓯᕆᔭᐅᑎᓪᓗᒋᑦ ᓇᑦᑏᑦ ᐱᑕᖃᐅᕐᓂᖏᑦ ᐊᒻᒪ ᐱᑕᖃᐅᕐᓂᐅᔪᓄᑦ ᐋᖅᑭᙳᐊᖅᑕᐅᓯᒪᔪᑦ ᐊᑐᖅᑕᐅᓪᓗᑎᒃ ᓇᓗᓇᐃᔭᖅᑕᐅᕐᑯᓪᓗᒋᑦ ᓇᑏᑦ ᓇᔪᖅᐸᒃᑕᖏ ᒥᒃᓴᐅᓵᖅᑕᐅᓪᓗᑎ, ᓇᑏᑦ ᐅᓄᕐᓂᖏᑦ ᑕᓯᐅᔭᕐᒥ ᑕᐃᑲᓂ 2008 1.3 ᓇᑎ ᑭᓚᒦᑕ/ᑭᑉᐹᓇᒃᑐᒥ 2018-ᒥ (ᐹᕙᓐᓛᓐ 2012) ᐊᕐᕋᒍᒥᑦ-ᐊᕐᕋᒍᒧᑦ ᐊᔾᔩᒃᑕᖃᑦᑕᙱᓐᓂᖏᑦ ᓇᑏᑦ ᐱᑕᖃᐅᕐᓂᖏᑦ ᑎᑎᕋᖅᑕᐅᓯᒪᖕᒥᔪᑦ ᐱᓇᖕᓇᖖᒑᖓᓄᑦ ᑕᓯᐅᔭᕐᔪᐊᑉ,

ᐊᒥᓲᓂᖏᓐᓄᑦ 2021-ᒥ ᐊᒻᒪ 2024-ᒥ ᓇᑦᑎᓂᕐᓂᒃ ᖃᖓᑕᓲᒃᑯᑦ ᖃᐅᔨᓴᕐᓂᕐᒧᑦ ᐱᓕᕆᐊᖅ (RSASP) ᓴᖅᑭᔮᖅᑎᑦᑎᓚᐅᖅᑐᑦ ᐊᕐᕋᒍᑕᓖᑦ ᐊᓯᔾᔨᖅᑕᕐᓂᖏᓐᓂᒃ ᐃᒃᐱᑭᑦᑐᕐᔪᐊᓂ. ᐃᒃᐱᑭᑦᑐᕐᔪᐊᓂ, ᓇᑏᑦ ᐊᒥᓲᓂᖏᑦ ᐅᓄᕈᓐᓂᖅᐸᓪᓕᖅᓯᒪᔪᑦ 0.9 ᓇᑏᑦ/ᑭᓐᒥᑕ ᑭᑉᐹᓇᒃᑐᓂ 2021-ᒥ 0.5 ᓇᑏᑦ/ᑭᓐᒥᑕ ᑭᑉᐹᓇᒃᑐᓂ 2024-ᒥ. ᑕᓯᐅᔭᕐᒥ, ᓇᑏᑦ ᐊᒥᓲᓂᖏᑦ ᐅᓄᕈᓐᓂᖅᐸᓪᓕᖅᓯᒪᔪᑦ 1.2 ᓇᑏᑦ/ᑭᓐᒥᑕ ᑭᑉᐹᓇᒃᑐᓂ 2021-ᒥ 0.7 ᓇᑏᑦ/ᑭᓐᒥᑕ ᑭᑉᐹᓇᒃᑐᓂ 2024-ᒥ. ᐊᑐᐃᓐᓇᐅᔪᑦ ᐃᒻᒪᕐᓂᓴᑦ ᖃᐅᔨᓴᕈᑎᕕᓃᑦ ᑕᐅᕗᖓ ᐃᒪᐃᓐᓇᓱᒋᓐᓈᔪᑦ ᑕᒪᒃᑯᐊ ᖃᓄᑎᒋᐅᓂᖏᑦ ᐊᕐᕋᒍᒥᑦ ᐊᕐᕋᒍᒧᑦ ᐊᔾᔩᒃᑕᖃᑦᑕᙱᓐᓂᖏᑦ ᑕᐃᒪᐃᒐᔫᒃᑐᙱᑦᑐᑦ ᐅᕝᕙᓘᓐᓃᑦ ᐊᔾᔨᐅᙱᑦᑑᖏᑦᑐᖅ ᑕᒪᒃᑯᓄᖓ ᐃᓂᐅᔪᓄᑦ (ᐹᕙᓐᓛᓐ 2012; ᔭᖕ ᐃᓘᓇᑎᒃ 2025). ᐱᒋᐊᕈᑕᐅᔪᑦ ᖃᐅᔨᓴᕈᑏᑦ ᑲᑎᑕᐅᓯᒪᔪᑦ 2006-ᒥ, 2007-ᒥ, ᐊᒻᒪ 2008-ᒥ ᓴᖅᑭᔮᖅᑎᑦᑎᖕᒥᔪᑦ ᐊᕐᕋᒍᑕᓖᑦ ᐊᓯᔾᔨᖅᑕᖃᑦᑕᕐᓂᖏᓐᓂᒃ ᐱᑕᖃᐅᕐᕕᐅᔪᓄᑦ ᓇᓚᐅᑦᑖᖅᑕᐅᓯᒪᔪᑦ ᐊᔾᔩᒃᑕᙱᓐᓂᖃᖅᓗᑎᒃ 0.2 ᓇᑏᑦ/ᑭᓐᒥᑕ ᑭᑉᐹᓇᒃᑐᓂ 2006-ᒥ, 1.6 ᓇᑏᑦ/ᑭᓐᒥᑕ ᑭᑉᐹᓇᒃᑐᓂ 2007-ᒥ ᐊᒻᒪ 0.7 ᓇᑏᑦ/ᑭᓐᒥᑕ ᑭᑉᐹᓇᒃᑐᓂ 2008-ᒥ (ᐹᕙᓐᓛᓐ 2012). ᒥᒃᓴᐅᓵᖅᑕᐅᓪᓗᑎ, ᓇᑏᑦ ᐅᓄᕐᓂᖏᑦ ᑕᓯᐅᔭᕐᒥ ᑕᐃᑲᓂ 2008 1.3 ᓇᑎ ᑭᓚᒦᑕ/ᑭᑉᐹᓇᒃᑐᒥ 2018ᒥᑦ (ᐹᕙᓐᓛᓐ 2012) ᐊᕐᕋᒍᒥᑦ-ᐊᕐᕋᒍᒧᑦ ᐊᔾᔩᒃᑕᖃᑦᑕᙱᓐᓂᖏᑦ ᓇᑏᑦ ᐱᑕᖃᐅᕐᓂᖏᑦ ᑎᑎᕋᖅᑕᐅᓯᒪᖕᒥᔪᑦ ᐱᓇᖕᓇᖖᒑᖓᓄᑦ ᑕᓯᐅᔭᕐᔪᐊᑉ, ᔮᖕ ᐃᓅᓐᓇᖅᒃ (2015) ᐅᔾᔨᕈᓯᓚᐅᖅᑐᑦ ᐊᑯᓂᐅᔪᒃᑯᑦ ᐅᓄᕈᓐᓂᖅᐸᓪᓕᐊᓯᒪᓂᖏᓐᓂᒃ ᐱᑕᖃᐅᕐᓂᐅᕕᑦ 1995-ᒥᑦ 2013-ᒧᑦ ᑕᐃᔭᐅᓯᒪᒐᓗᐊᖅᑎᓪᓗᒋᑦ ᐊᕐᕋᒍᒥᑦ ᐊᕐᕋᒍᒧᑦ ᐊᓯᔾᔨᖅᑕᖃᑦᑕᕐᓂᐅᔪᑦ. ᑕᐃᒪᐃᓐᓂᖓᓄᑦ, ᕿᒥᕐᕈᓂᖅ ᐊᕐᕋᒍᒥᑦ-ᐊᕐᕋᒍᒧᑦ ᖃᓄᐃᓐᓂᖅᓴᐅᖕᒪᖔᑕ ᕿᒥᕐᕈᓂ ᓂᕐᔪᑏᑦ ᐊᒥᓲᓂᖏᓐᓂᒃ ᓄᓇᖓᓂ ᓈᒻᒪᙱᑐᐃᓐᓇᓇᐊᓕᒃ ᕿᒥᕐᕈᑎᓪᓗᒋᑦ ᐅᒥᐊᕐᔪᐊᓄᑦ-ᐊᒃᑐᐊᔪᓄᑦ ᐊᒃᑐᐃᓂᕐᓂᒃ ᓇᑦᑎᕐᓄᑦ, ᐃᓚᓕᐅᑎᓯᒪᓪᓗᑎᒃ ᓈᒻᒪᒃᑐᒥᒃ ᖃᐅᔨᒋᐊᕐᕕᐅᔪᓐᓇᖅᑐᑦ ᐃᓅᑦ (ᓲᕐᓗ ᑕᓯᐅᔭᖅ) ᖃᐅᔨᓴᕈᑏᑦ ᐋᖅᑭᒃᓯᒪᓂᖏᓐᓄᑦ ᐱᔪᓐᓇᖅᓯᑎᑦᑎᓯᒪᔪᖅ ᐊᒃᑐᐃᓂᕐᒥᒃ ᐱᒋᐊᖅᑳᖅᑎᓐᓇᒍ-ᐱᓕᕆᓕᖅᑎᓪᓗᒋᑦ/ᖃᐅᔨᒋᐊᕐᕕᐅᔪᓐᓇᖅᑐᓄᑦ-ᐊᒃᑐᐃᓃᑦ (BACI) ᕿᒥᕐᕈᓂᖅ ᐊᒃᑐᐃᓂᐅᑐᐃᓐᓇᕆᐊᓕᖕᓂ ᐅᒥᐊᕐᔪᐊᖃᖃᑦᑕᕐᓂᕐᒥ ᓇᑦᑎᕐᓄᑦ ᐊᔾᔨᙱᑦᑕᕐᔪᐊᕋᓗᐊᖅᑎᓪᓗᒋᑦ ᖃᐅᔨᓴᕈᑏᑦ ᑖᒃᑯᓇᓂ ᖃᐅᔨᓴᕐᓂᕐᒧᑦ ᐊᕐᕋᒎᔪᓂ. ᑖᓐᓇ ᒫᓐᓇ ᐅᓂᒃᑳᖅ ᐋᖅᑭᒃᓯᓯᒪᔪᖅ ᐱᒋᐊᕈᑕᐅᔪᓄᑦ ᖃᐅᔨᓴᕈᑏᑦ ᖃᓄᐃᓕᖓᓂᖏᓐᓄᑦ ᓇᑦᑎᕐᓄᑦ ᐅᐊᖕᓇᖓᓄᑦ ᐊᒥᑦᑑᑉ ᐃᒪᖓᓂ, ᐱᖃᓯᐅᑎᓪᓗᒋᑦ ᓇᓗᓇᐃᕈᑏᑦ ᓇᑏᑦ ᐱᑕᖃᐅᕐᓂᖏᓐᓄᓂᑦ ᐃᒃᐱᑭᑦᑐᕐᔪᐊᓂ, ᓈᓴᐅᑕᐅᓚᐅᒃᑐᑦ, 20-30%-ᐸᓗᖕᒥᒃ ᐅᓗᕆᓐᓂᖅᓴᐅᓚᐅᓗᐊᖅᑎᓪᓗᒋᑦ ᑖᒃᑯᐊ ᖃᐅᔨᒋᐊᕐᕕᐅᔪᓐᓇᖅᑐᓂ ᐃᓂᓂ ᑕᓯᐅᔭᕐᒥ. ᑕᒪᓐᓇ ᑐᓴᐅᒪᔾᔪᑎ ᐊᑐᐃᓐᓇᕈᐃᓯᒪᔪᖅ ᒪᓕᒃᑕᐅᔪᓐᓇᖅᑐᒥᒃ ᖃᐅᔨᓴᖅᐸᓪᓕᐊᖏᓐᓇᕐᓂᕐᒧᑦ ᓄᓇᓂ ᐊᕙᒃᑐᖅᓯᒪᔪᓂ ᐊᓯᔾᔨᐅᑎᓄᑦ ᓇᑦᑎᕐᓄᑦ ᐊᒃᑐᐊᓂᓖᑦ ᐊᒥᓲᓂᖏᓐᓄᑦ ᐃᓱᒪᒋᓪᓗᒋᑦ ᐹᕙᓐᓛᓐᑯᑦ ᓯᕗᓂᒃᓴᒥ ᐅᒥᐊᕐᔪᐊᖃᖃᑦᑖᕐᓂᖏᑦ.

ᖄᖕᒐᓂ ᐱᑕᖃᐅᕐᓂᐅᔪᓄᑦ ᐋᖅᑭᙳᐊᖅᑕᐅᓯᒪᔪᓂᒃ ᐊᑐᖅᓱᑎᒃ, ᓇᑦᑏᑦ ᐱᑕᖃᕐᕕᖕᖏᑦ ᓇᓗᓇᐃᖅᑕᐅᓯᒪᖕᒥᔪᑦ ᐃᒃᐱᑭᑦᑐᕐᔪᐊᓂ ᐊᒻᒪ ᑕᓯᐅᓴᕐᒥ 2021-ᒥ ᐊᒻᒪ 2024-ᒥ. ᐱᑕᖃᕐᕕᖕᖏᓐᓂᒃ ᕿᒥᕐᕈᓂᖅ ᒫᓐᓇᓚᐅᑲᒃ ᐊᓯᔾᔨᕐᓂᐅᔪᓂᒃ ᐊᔾᔨᒋᙱᔾᔪᑎᖕᖏᓐᓂᓪᓗ ᐱᑕᖃᕐᕕᖕᖏᓐᓂ ᓇᓃᑉᐸᖕᓂᖕᖏᓐᓄᑦ ᖃᓄᑎᒋᐅᓂᖕᖏᓪᓗ ᐃᒃᐱᑭᑦᑐᕐᔪᐊᓂ ᑕᓯᐅᓴᕐᒥᓗ. ᐃᒃᐱᑭᑦᑐᕐᔪᐊᓂ, ᐊᖕᒋᔪᒥᒃ ᑐᔾᔭᐱᒃᑐᑦ ᐱᑕᖃᕐᕕᖕᖏᑦ ᑖᒃᑯᓇᓂ ᐊᕐᕌᒍᓂ 51.6 ᑭᓛᒥᑕᑦ ᑭ<ᐹᓇᒃᑯᑦ, ᑭᒻᒐᖅᑐᐃᓪᓗᑎᒃ 12.2%-ᒥᒃ ᐊᒻᒪ 9.9%-ᒥᒃ ᑲᑎᕝᓗᒋᑦ ᐱᑕᖃᕐᕕᖕᖏᓐᓂ ᐃᓅᑦ 2021-ᒥ ᐊᒻᒪ 2024-ᒥ. ᐃᓱᒪᒋᓪᓗᒋᑦ, ᑕᓯᐅᓴᕐᒥ ᐊᖕᒋᔪᒥᒃ ᑐᔾᔭᐱᒃᑐᑦ ᐱᑕᖃᕐᕕᖕᖏᓐᓂ ᑖᒃᑯᓇᓂ ᐊᕐᕌᒍᓂ 151.0 ᑭᓛᒥᑕᑦ ᑭ<ᐹᓇᒃᑐᑦ, ᑭᒻᒐᖅᑐᐃᓪᓗᓂ 39.2% ᐊᒻᒪ 40.7% ᑲᑎᕝᓗᒋᑦ ᐱᑕᖃᕐᕕᖕᖏᑦ ᐃᓅᑦ 2021-ᒥ ᐊᒻᒪ 2024-ᒥ, ᐃᓱᒪᒋᔭᐃᓐᓇᓇᓪᓗᒋᑦ. ᑕᒪᒃᑯᐊ ᐃᓕᖅᑯᓯᐅᓕᖅ<ᒃᑐᑦ ᐃᒪᐃᓐᓇᓱᒋᓐᓈᔪᑦ ᑕᒪᓐᓇ ᐋᖅᑭᒃᓯᒪᓂᖕᒋᑦ ᐱᑕᖃᕐᕕᖕᖏᓐᓄᑦ ᐊᓯᔾᔨᖅᑕᖅᑑᓂᖕᒐᓂᒃ ᐃᓚᖕᒐᒍᑦ ᐊᒻᒪ ᐊᒃᑐᖅᑕᐅᓯᒪᔫᒃᓴᐅᔪᑦ ᐊᕙᑎᒥ ᐱᔾᔪᑕᐅᕙᒃᑐᓂᒃ ᑕᐃᔅᓯᒪᓂᐅᑎᓪᓗᒍ ᐊᕐᕌᒍᐊᓂ.

ᑕᒪᐃᓐᓄᑦ, ᓇᑦᑎᕐᓂᒃ ᖃᖕᒐᑕᓲᒃᑯᑦ ᖃᐅᔨᓴᕐᓂᕐᒧᑦ ᐱᓕᕆᐊᒥ (RSASP) ᖃᐅᔨᔭᐅᔪᑦ ᓇᓗᓇᐃᖅᓯᔪᑦ ᑖᒃᑯᐊ ᓇᑦᑏᑦ ᐱᑕᖃᐅᕐᓂᖕᒋᑦ ᐃᒃᐱᑭᑦᑐᕐᔪᐊᓂ ᐱᓕᕆᕝᕕᐅᓇᔭᖅᑐᒥ ᓴᖅᑮᔭᖅᑎᑦᑐᑎᔪᑦ ᑕᐃᒪᐃᓕᖕᒐᓂᑐᐃᓐᓇᐅᕙᒃᑐᓂᒃ ᐊᖕᒋᔪᑎᒍᑦ ᐊᒻᒪ ᒫᓐᓇᓚᐅᑲᒃ ᐊᓯᔾᔨᖅᑕᖅᑐᑦ ᐃᓱᒪᒋᖃᓯᐅᔾᔭᐅᔭᓇᐊᓖᑦ ᓇᓕᐊᖕᓂᑐᐃᓐᓇᖅ ᓯᕗᓂᒃᓴᒥ ᖃᐅᔨᓴᕐᓂᕐᒧᑦ ᐋᖅᑭᒃᓯᒪᓂᐅᔪᓂ ᑐᕌᒐᖃᖅᑐᑦ ᕿᒥᕐᕈᓂᕐᒥᒃ ᐅᒥᐊᕐᔪᐊᓂ ᐊᒃᑐᐃᓂᐅᑐᐃᓐᓇᓇᐊᓕᖕᓂ ᓇᑦᑎᕐᓄᑦ. ᒫᓐᓇ ᖃᐅᔨᓴᕐᓂᖅ ᓴᙱᒃᑎᒋᐊᖅᑎᑦᑎᕙᒃᐳᖅ ᐱᒻᒪᕆᐅᔪᓂᒃ ᓴᖅᑮᓂᕐᒧᑦ ᐊᑯᓂᐅᔫᒃᑯᑦ ᖃᐅᔨᓴᕈᑎᓂᒃ ᐱᒋᐊᕈᑕᐅᔪᑦ ᖃᐅᔨᓴᕈᑏᑦ ᖃᓄᐃᓕᖕᒐᓂᖕᒋᓐᓄᑦ ᐊᒻᒪ ᐅᔭᕆᖕᓂᐊᕐᕕᖕᒧᓪᓚᑦᑖᖅᑐᑦ ᖃᔭᓴᕈᑎᓂᒃ ᑲᑎᑦᑎᓂᖅ, ᖃᐅᔨᓴᖅ<ᓪᓕᐊᖕᒋᓐᓇ<ᓂ<ᒥ ᖃᐅᔨᔭᐅᔪᑦ ᓈᒻᒪᒃᑐᒃᑯᑦ ᐃᓚᓕᐅᔾᔭᐅᓯᒪᓗᑎᒃ ᐱᓕᕆᐊᓇᔭᐅᕐᔪᐊᖅᓯᒪᔪᓄᑦ ᖃᐅᔨᒋᐊᕈᑎᓄᑦ ᖃᐅᔨᖅ<ᓪᓕᐊᖕᒋᓐᓇᕐᓂᕐᒧᑦ ᐱᓕᕆᓂᕐᓄᑦ (ᓲᕐᓗ ᐊᒃᑐᐃᓂᕐᓄᑦ ᖃᐅᔨᓴᖅ<ᓪᓕᐊᖕᒋᓐᓇᕐᓂᕐᒧᑦ ᐱᓕᕆᐊᑦ ᖃᐅᔨᓴᕐᓂᑦ) ᐊᒻᒪ ᐋᖅᑭᒡᕕᖃᐃᓐᓇᖅᑐᒥᒃ ᐊᐅᓚᑦᑎᓂᕐᒧᑦ <ᕐᓇᐅᑏᑦ ᐆᒃᑐᕋᖅᑕᐅᔪᓐᓇᕐᓱᑎᒃ ᐊᒃᑐᐃᓃᑦ ᓇᓗᐃᒃᑯᑕᖕᒋᑦ, ᖁ<ᕙᓯᓕᓇᑦ ᖃᓄᐃᓪᓕᔪᖃᖅᑳᖅᑎᓐᓇᒍ ᑭᒻᓕᐅᔪᑦ ᐊᒻᒪ ᐊᒃᑐᐊᓂᓖᑦ ᐊᐅᓚᑦᑎᓂᕐᒧᑦ ᐱᓕᓈᑦ ᐊᑐᓕᖅᑎᑦᑎᓂᕐᒧᑦ ᐊᒃᑐᐃᓈᑦ ᐅᖕᒐᑕᐅᔾᔨᓯᒪᓂᕈᑎᒃ ᒥᒃᓴᐅᓴᒃᑕᐅᔪᑦ ᖃᓄᑎᒋᐅᓂᖕᖏᓐᓄᑦ. ᑭᖑᓂᐊᒍᑦ ᐱᒋᐊᓚᐅᖅᑎᓪᓗᒋᑦ ᐅᒥᐊᕐᔪᐊᖃᖃᑦᑕᕐᓃᑦ ᑕᐅᕚᓇ ᓂᒋᐊᒍᑦ ᐅᒥᐊᕐᔪᐊᑦ ᐊᖅᑯᑖᒍᑦ, ᖃᐅᔨᓴᖅ<ᓪᓕᐊᖕᒋᓐᓇᕐᓂᖅ ᐊᑐᓕᖁᔭᐅᓯᒪᔪᖅ ᑲᑐᔾᔨᖃᑎᖃᕐᓱᑎᒃ ᖃᐅᔨᓴᖅ<ᓪᓕᐊᖕᒋᓐᓇᕐᓂᕐᒧᑦ ᐱᒋᐊᖅᑕᐅᓯᒪᔪᑦ ᑲᒪᒋᔭᐅᓪᓗᑎᒃ ᐊᒃᑐᐊᓂᓕᖕᓄᑦ ᒪᓕᒐᖅᑎᒍᑦ ᑐᑦᑕᕐᕕᐅᔪᓂ, ᐋᑐᑎᖃᑎᐊᖅᑐᒥᒃ ᖃᐅᔨᓴᖅ<ᓪᓕᐊᖕᒋᓐᓇᖅᑯᓪᓗᒋᑦ ᐊᒃᑐᐃᓂᐅᑐᐃᓐᓇᓇᐊᓕᖕᓂᒃ ᐅᒥᐊᕐᔪᐊᖃᖃᑦᑕᕐᓂᕐᒥᑦ ᓄᓇᖁᑖᓂ ᓇᑦᑏᑦ ᐊᒥᕉᓂᖕᒋᓐᓄᑦ, ᐱᖃᓯᐅᑎᓪᓗᒋᑦ ᑲᑎ<ᓪᓕᐊᑐᐃᓐᓇᓇᐊᓖᑦ ᐊᒃᑐᐃᓅᑦ ᐱᓗᐊᖅᑐᒥᒃ ᐊᑐᖅᓱᒋᑦ ᓯᕗᓂᒃᓴᒥ ᓯᓚᐅᒧᑦ ᐋᖅᑭᙳᐊᖅᑕᐅᓯᒪᔪᑦ ᐊᓯᔾᔩᑐᐃᓐᓇᓇᐊᓖ ᑕᓇᐅ< ᓯᑯᖕᒐᑕ ᖃᓄᐃᓕᖕᒐᓂᒋᕙᒃ ᑕᖕᒐᓄᑦ, ᓇᔪᒐᐃᑦ ᖃᓄᐃᓕᖕᒐᓂᖕᒋᓐᓄᑦ ᐊᒻᒪ/ᐅᕝᕙᓘᓐᓃᑦ ᐊᖑᓇᓱᒃᑕᐅᕙᒃᑐᑦ ᖃᓄᐃᓕᖕᒐᓂᓇᕙᒃᑕᓂ ᑕᐅᕙᓂ ᓄᓇᖁᑖᓂ.

Executive Summary

The ringed seal aerial survey program (RSASP) was conducted by WSP in the Foxe Basin region of the Southern Shipping Route in June 2021 and 2024. The primary objective of the surveys was to update baseline data on ringed seal density and distribution in the landfast ice area of the Southern Shipping Route in Steensby Inlet and in a control location (Tasiujaq). The secondary objective of the surveys was to identify ringed seal hotspots in the landfast ice areas of Steensby Inlet and Tasiujaq.

Two types of analyses were performed on the 2021 and 2024 datasets. Strip-transect analysis of infrared imagery combined with digital photographs was used to calculate ringed seal densities and density surface modelling was used to identify ringed seal hotspots.

Results of the 2021 and 2024 RSASP show pronounced yearly fluctuations in ringed seal density in Northern Foxe Basin. In Steensby Inlet, ringed seal density decreased from 0.9 seals/km² in 2021 to 0.5 seals/km² in 2024. In Tasiujaq, ringed seal density decreased from 1.2 seals/km² in 2021 to 0.7 seals/km² in 2024. Available historical data for the region suggests that this level of inter-annual variability is not uncommon nor unique to these locations (Baffinland 2012; Young et al. 2015). Baseline data collected in 2006, 2007 and 2008 also showed yearly fluctuations in ringed seal density in Steensby Inlet, ranging from 0.2 seal/km^2 in 2006, 1.6 seals/km^2 in 2007 to 0.7 seal/km^2 in 2008 (Baffinland 2012). In comparison, ringed seal density in Tasiujaq during 2008 was 1.3 seals/km^2 in 2008 (Baffinland 2012). Year-to-year variation in ringed seal densities has also been documented in western Hudson Bay, where Young et al. (2015) observed a long-term decline in densities from 1995 to 2013 amidst pronounced interannual fluctuations. As a result, looking exclusively at year-to-year comparisons of animal density in the region may not be suitable for evaluating shipping-related effects on ringed seal. Integrating a suitable control site (i.e., Tasiujaq) into the study design allows for an effective before-after/control-impact (BACI) assessment of potential shipping effects on ringed seal despite high data variability between survey years. The present report establishes baseline conditions for ringed seals in Northern Foxe Basin, including evidence that ringed seal density in Steensby Inlet is, on average, approximately 20–30% lower than that in the control site at Tasiujaq. This information provides a basis for monitoring potential regional changes in ringed seal relative abundance in relation to Baffinland's future shipping activities.

Using surface density models, the present study has also identified ringed seal hotspots in Northern Fox Basin, including shifts in hotspot distribution and hotspot size between survey years and survey strata. In Steensby Inlet, the spatial overlap of hotspots between survey years was 51.6 km^2, representing 12.2% and 9.9% of the total hotspot areas in 2021 and 2024, respectively. In Tasiujaq, the spatial overlap of hotspots between survey years was 151.0 km², representing 39.2% and 40.7% of the total hotspot areas in 2021 and 2024, respectively. These patterns suggest that the establishment of hotspots is somewhat dynamic and likely influenced by environmental factors at play in that given year.

Overall, the RSASP results indicate that ringed seal density in the Steensby Project area exhibits natural spatial and temporal variability that must be considered in any future study design aimed at evaluating potential shipping impacts on ringed seals. The present study reinforces the importance of establishing a long-term dataset for baseline conditions and site-specific data collection, where monitoring results should be appropriately integrated into a robust follow-up monitoring program (i.e., EEM study) and adaptive management plan with measurable effect indicators, tiered thresholds and associated management actions for implementation should impacts

exceed predicted levels. Following the start of shipping activities along the Southern Shipping Route, continued monitoring is recommended in collaboration with ongoing monitoring initiatives led by the relevant regulatory agencies, in order to effectively monitor for potential shipping effects on the local ringed seal population, including potential cumulative effects, particularly under future climate scenarios that may alter sea ice regimes, habitat conditions and/or prey dynamics in the region.

Study Limitations

WSP Canada Inc. has prepared this document in a manner consistent with that level of care and skill ordinarily exercised by members of the engineering and science professions currently practising under similar conditions in the jurisdiction in which the services are provided, subject to the time limits and physical constraints applicable to this document. No warranty, express or implied, is made.

This document, including all text, data, tables, plans, figures, drawings and other documents contained herein, has been prepared by WSP for the sole benefit of Baffinland Iron Mines Corporation (Baffinland). The Executive Summary was translated into Inuktitut and provided by Baffinland to WSP. In the event of discrepancies in information or interpretation, the English version shall prevail. This report represents WSP's professional judgement based on the knowledge and information available at the time of completion. WPS is not responsible for any unauthorized use or modification of this document. All third parties relying on this document do so at their own risk.

The factual data, interpretations, suggestions, recommendations, and opinions expressed in this document pertain to the specific project, station conditions, design objective, development and purpose described to WSP by Baffinland, and are not applicable to any other project or station location. In order to properly understand the factual data, interpretations, suggestions, recommendations and opinions expressed in this document, reference must be made to the entire document.

This document, including all text, data, tables, plans, figures, drawings, and other documents contained herein, as well as all electronic media prepared by WSP, is considered it's professional work product and shall remain the copyright property of WSP. Baffinland may make copies of the document in such quantities as are reasonably necessary for those parties conducting business specifically related to the subject of this document or in support of or in response to regulatory inquiries and proceedings. Electronic media is susceptible to unauthorized modification, deterioration, and incompatibility, and therefore, no party can rely solely on the electronic media versions of this document.

.

Table of Contents

TABLES

FIGURES

APPENDICES

Abbreviation and Acronym List

AIC	Akaike's Information Criterion
ASL	Above sea level
Baffinland	Baffinland Iron Mines Corporation
°C	Degrees Celsius
χ^2	Chi-square goodness-of-fit tests
CI	Confidence Interval
CV	Coefficient of Variation
DSM	Density surface modelling
ECMWF	European Centre for Medium-Range Weather Forecasts
edf	Effective degrees of freedom
EEM	Environmental Effects Monitoring
ERP	Early Revenue Phase
FEIS	Final Environmental Impact Statement
FLIR	Forward-looking Infrared Camera
ft	Feet
Gi*	Getis-Ord Gi*
GAM	Generalized Additive Model
GPS	Global Positioning System
IBCAO	International Bathymetric Chart of the Arctic Ocean
IQ	Inuit Qaujimajatuqangit
km	Kilometres
km^2	Square kilometres
km/h	Kilometres per hour
LSA	Local Study Area
maxD	Maximum depth
MCDS	Multiple covariate distance sampling

MEWG	Marine Environmental Working Group
Milne Port	Port at Milne Inlet
minD	Minimum depth
minDist	Minimum distance to shore or floe edge
MMP	Marine Monitoring Program
Mtpa	Million tonnes per annum
NIRB	Nunavut Impact Review Board
Project	Mary River Project
PC	Project Certificate No. 005
QQ	quantile-quantile plots
QIA	Qikiqtani Inuit Association
REML	Restricted maximum likelihood
RSA	Regional Study Area
RSASP	Ringed Seal Aerial Survey Program
s	Univariate smooth
so	Soap-film spatial smooth
SE	Standard Error
ShrDst	Distance to shore
Steensby Port	Port at Steensby Inlet
te	Bivariate tensor smooth

1.0 INTRODUCTION

This report presents the results of the 2021 and 2024 Ringed Seal Aerial Survey Program (RSASP) conducted in Northern Foxe Basin, Nunavut. During the molting season in early June, ringed seal density and distribution in Steensby Inlet (study area) and Tasiujaq (control area) were estimated using infrared and high-resolution photographic imagery collected during systematic aerial surveys undertaken in this region following a strip-transect survey design. The primary objective of the RRASP was to characterize ringed seal density and distribution in the proposed footprint of a future port facility and shipping route in Northern Foxe Basin, including identification of ringed seal hotspots in this region during the ice-covered period.

1.1 Project Background

The Mary River Project (hereafter, “the Project”) is an operating open-pit iron ore mine owned by Baffinland Iron Mines Corporation (Baffinland) and located in the Qikiqtani Region of North Baffin Island, Nunavut (Figure 1). The operating mine site is currently connected to Milne Port, located at the head of Milne Inlet, via the 100 km long Tote Road. An approved but yet-undeveloped component of the Project includes a South Railway connecting the Mine Site to an undeveloped port at Steensby Inlet (Steensby Port).

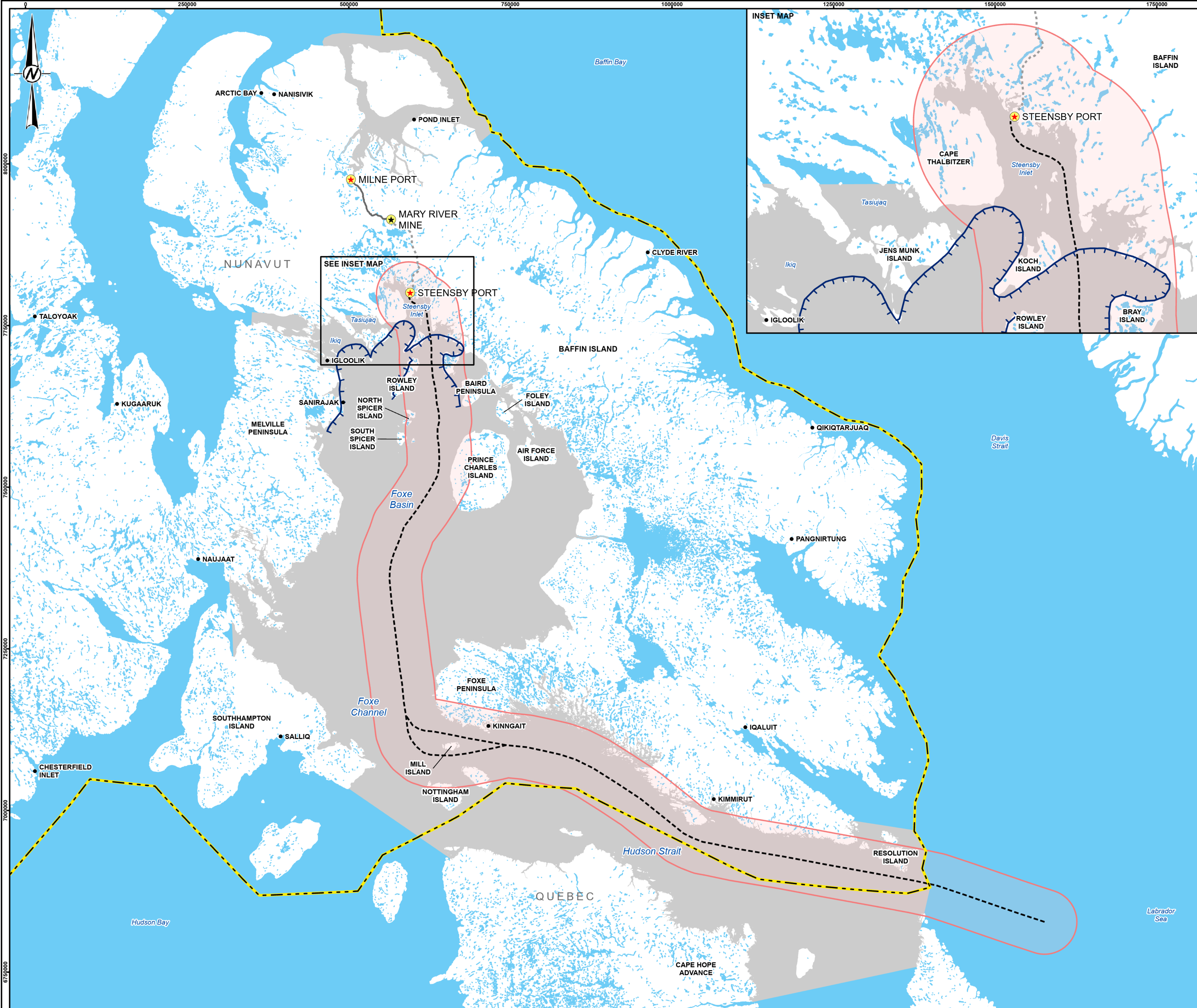

LEGEND

- COMMUNITY
- MARY RIVER MINE
- PORT LOCATION
- FLOE EDGE - IQ (BAFFINLAND 2012B,F)
- HAUL ROAD
- PROPOSED RAILWAY
- SHIPPING ROUTE (APPROXIMATE)
- LOCAL STUDY AREA
- MARINE REGIONAL STUDY AREA
- NUNAVUT SETTLEMENT BOUNDARY
- WATERBODY

0 250 500

1:6,000,000 KILOMETRES

REFERENCE(S)

BASE DATA OBTAINED FROM GEOGRATIS, © DEPARTMENT OF NATURAL RESOURCES CANADA. ALL RIGHTS RESERVED. SHIPPING ROUTE PROVIDED BY CLIENT, JUNE 8, 2022. NUNAVUT SETTLEMENT BOUNDARY OBTAINED FROM NUNAVUT TUNNGAVIK INC., OCTOBER 9, 2012. PROJECTED COORDINATE SYSTEM: NAD 1983 UTM ZONE 17N

CLIENT
BAFFINLAND IRON MINES CORPORATION

PROJECT
MARY RIVER PROJECT
2021 & 2024 RINGED SEAL AERIAL SURVEYS

TITLE
PROJECT LOCATION

CONSULTANT

YYYY-MM-DD	2025-10-28
DESIGNED	TT
PREPARED	AA
REVIEWED	TT
APPROVED	PA

PROJECT NO.	CONTROL	REV.	FIGURE
CA0051512.6683	1000.01	0	1

IF THIS MEASUREMENT DOES NOT MATCH WHAT IS SHOWN, THE SHEET SIZE HAS BEEN MODIFIED FROM: ANSI B

1.2 Regulatory Drivers

In accordance with existing Terms and Conditions of Nunavut Impact Review Board (NIRB) Project Certificate (PC) No. 005, Baffinland is responsible for the establishment and implementation of the Marine Monitoring Plan (MMP), which comprises environmental effects monitoring studies that are conducted over a sufficient time to allow for the following objectives:

- To measure the relevant effects of the Project on the marine environment.
- To confirm that the Project is being carried out within the pre-determined terms and conditions relating to the protection of the marine environment.
- To assess the accuracy of the predictions contained in the Final Environmental Impact Statement (FEIS) for the Project.

The RSASP is one of several monitoring programs that collectively make up the MMP for marine mammals. The RSASP was designed to address PC conditions related to evaluating potential disturbance to ringed seals from shipping activities that may result in changes in animal distribution, abundance, and migratory movements in the study area. Specifically, this included the following PC conditions:

- Term and Condition No. 99 – "*The Proponent, working with the Marine Environment Working Group, shall consider and identify priorities for conducting the following supplemental baseline assessments:*
  - *c. Enhance baseline data on marine wildlife (fish, invertebrates, birds, mammals, etc.) and to provide more details on species abundance and distribution found in the Project area. This shall include, but not be limited to the following:*
    - *iii. Aerial surveys for basking ringed seals throughout the landfast ice of Steensby Inlet and at an appropriate control location*
- Term and Condition No. 101 - *"The Proponent shall incorporate into the appropriate monitoring plans the following items:*
  - *b. Efforts to involve Inuit in monitoring studies at all levels.*
  - *c. Monitoring protocols that are responsive to Inuit concerns.*
  - *e. Schedule for periodic aerial surveys as recommended by the Marine Environment Working Group (MEWG)."*
  - *f. Periodic aerial surveys for basking ringed seals throughout the landfast ice of Steensby Inlet, and a suitable control location. Surveys shall be conducted at an appropriate frequency to detect change in inter-annual variability;*
- Term and Condition No. 109 - *"The Proponent shall conduct a monitoring program to confirm the predictions in the FEIS with respect to disturbance effects from ships noise on the distribution and occurrence of marine mammals. The survey shall be designed to address effects during the shipping seasons, and include locations in Hudson Strait and Foxe Basin, Milne Inlet, Eclipse Sound and Pond Inlet. The survey shall continue over a sufficiently lengthy period to determine the extent to which habituation occurs for narwhal, beluga, bowhead and walrus".*

- Term and Condition No. 111 - *"The Proponent shall develop clear thresholds for determining if negative impacts as a result of vessel noise are occurring".*
- Term and Condition No. 119 - "In conjunction with the MEWG, monitor ringed seal birth lair abundance and distribution for at least two years prior to the start of ice-breaking to develop a baseline, with continue monitoring over the life-time of the project*".*
- Term and Condition No. 126 - *"The Proponent shall design monitoring programs to ensure that local users of the marine area in communities along the shipping route have opportunity to be engaged throughout the life of the Project in assisting with monitoring and evaluating potential project-induced impacts and changes in marine mammal distributions".*

1.3 Adaptive Management Protocol

Adaptive management is a planned and systematic process for continuously improving environmental management practices by learning about their outcomes (CEAA 2009). Adaptive management provides flexibility to identify and implement new mitigation measures or to modify existing ones during the life of a project. Adaptive strategies are implemented when unanticipated adverse effects are observed or if effects exceed identified thresholds.

In support of Baffinland's Phase 2 Proposal for the Project, Baffinland developed a draft Adaptive Management Plan (AMP), which provides a framework for how adaptive management is incorporated into Project operations (Baffinland 2020b). As part of this process, a Marine Mammal Trigger Action Response Plan (TARP) was developed for the Project, which identified several performance indicators, effect thresholds and pre-defined actions (i.e., responses) that are used to evaluate and respond to potential Project effects on marine mammal species in the Project area (Baffinland 2021). The TARP uses a broad range of effect indicators that are measured against a series of tiered thresholds (i.e., low, moderate and high-risk thresholds) that are designed to guide short-term and long-term adaptive management strategies. The pre-defined actions identified in the TARP describe the responses that Baffinland would implement should the corresponding threshold levels be exceeded, assuming there is a degree of certainty that the measured change is Project-related. Three levels of action have been identified: low, moderate, and high. These responses include but are not limited to increased monitoring and data analysis (e.g., trend analysis), identification of possible sources, and risk assessment and/or mitigation. Baffinland released the most current version of the Marine Mammal TARP and Action Toolkits as part of the draft MMP submitted to the NIRB on 15 May 2023 (Baffinland 2023b).

The following criterion relevant to ringed seal in the Project area has been identified, which represents a 'High Risk' threshold for ringed seal:

- Confirmed[1] >25.0% decrease in density throughout the Local Study Area (LSA).

In the event that this threshold criterion is exceeded following the start of shipping operations in Steensby Inlet, a pre-determined 'High Risk' response would be triggered, as defined in Baffinland (2023b).

[1] Confirmed indicates that the Risk Status/ Threshold trigger has been observed in at least two consecutive monitoring programs, whether during the regular monitoring schedule or confirmed through a special study.

1.4 Ringed Seal Background

Ringed seals (*Pusa hispida*) have a circumpolar distribution and are found in all seasonally ice-covered seas of the Northern Hemisphere. Ringed seals that occur within Canadian waters are found throughout the Arctic Ocean, Beaufort Sea, Hudson Bay, Hudson Strait, Baffin Bay, Labrador Sea, and Canadian Arctic Archipelago (COSEWIC 2019).

The population structures of ringed seals across the Canadian Arctic are poorly understood in general. The ringed seal population in Canada and adjacent waters (West Greenland, Alaska, and Russia) is estimated at 2.3 million seals, with low confidence (COSEWIC 2019). Smith (1975) estimated the Hudson Bay and James Bay regions to have approximately 516,000 ringed seals, although this estimate does not include Foxe Basin. No population estimate has been calculated for the Foxe Basin area.

Young et al. (2015) reported on data from systematic aerial strip transect surveys flown in western Hudson Bay in late May to early June of 1995–1997, 1999, 2000, 2007–2010 and 2013. The same 10 transects from the Hudson Bay shoreline in the west to the 89° W longitude line in the east, and from Churchill, Manitoba, to Arviat, Nunavut, were surveyed. The density of hauled-out ringed seals ranged from 1.22 seals/km^2 in 1995 to 0.20 seals/km^2 in 2013. Yearly density estimates varied significantly but suggested a gradual decline in seal density from 1995 to 2013 (Young et al. 2015; Ferguson et al. 2017). Ferguson et al. (2017) concluded that although negative demographic responses were gradually occurring with sea ice declines in Hudson Bay, an episodic environmental event (the year 2010 was the earliest spring break-up and the latest ice formation in Hudson Bay, which coincided with high cortisol levels and declines in reproductive rates) may have played a significant role in a punctuated decline observed in 2013. The results may provide evidence of changes in the condition of ringed seals (i.e., ovulation rate, pregnancy rate, stress levels, and sick seals) in relation to climate-mediated sea ice dynamics (Ferguson et al. 2017).

Based on best available science (McLaren 1958; Smith and Stirling 1975; Smith and Hammill 1981; Smith 1987; Hammill et al. 1991; Lyderson 1995; Kelly et al. 2010; Chambellant et al. 2012a), the breeding season for ringed seal, which includes pupping, nursing and mating, occurs in the Eastern High Arctic between March and May, with mating occurring towards the end of the nursing period and preceding the annual molt in June, when ringed seals haul out on ice to bask in the sun (McLaren 1958; Smith 1973a). Furgal et al. (2002) further indicated pupping occurred from late March until early April, when females inhabit haul-out lairs and birth white-coated pups (McLaren 1958; Smith & Stirling 1975; Kingsley 1990; Smith & Hammill 1981).

Inuit Qaujimajatuqangit (IQ) reported in JPCS (2017) and ERM (2019) indicated that the seal pupping season runs from February to March, and as late as the middle of April and May, throughout the regional study area (RSA). Additionally, IQ recorded in QIA (2019) provided additional knowledge regarding the areas in which seal pupping takes place. The following is a summary of IQ from these resources:

> *"…seal hunting also continues in Ukiuq and seal pupping will last into March. Ringed seal pups are preferred by local Inuit and are harvested throughout Eclipse Sound*." - p. 32, JPCS 2017.

> *"Starting in March the seal pups are born. March and June are the most important months. In the past, it didn't used to be until April that the seals were born. Just to the west of us now, they are catching pups. March and June are the months I'm worried about. Most able men go out still, even if it's just occasionally."* – Workshop #2 Participant, 27-29 April 2015, p. 48, JCPS 2017.

> *"There are seal pups in the area until the middle of April."* – Elijah, 27-29 April 2015, p.165, JCPS 2017.

"There are no certain areas for seal pups; they are born everywhere. Even along the routes we travel. That is something that needs to be monitored." - Paniloo, 27-29 April 2015, p. 171, JPCS 2017.

"We have to give consideration to seals when they start giving birth in April and May. In May, they are quite large and some seal pups…" – Elijah, 27-29 April 2015, p. 178, JPCS 2017.

"The baby seals breed in March..." Sakiasee, 27-29 April 2015, p. 217, JPCS 2017.

"In the spring (March to May), seal pups are very small and vulnerable…" – Workshop #3 Participant, p. 17, ERM 2019).

"…So the seals come in to the Eclipse Sound to feed and mate. So, they come in from offshore, and he says in March they start coming in to this area, March, April, May and they'll just keep going in to the sounds." – Participant 11, 05 February 2019, p. 43, QIA 2019.

"…Also, regular movement of the seals around here all the time, and moving up there, especially in Eclipse Sound Area they, which is part of the, those inlets, Milne and Tremblay Sound at almost every inlet these are seal calving areas. When the ice break up in the middle of the summertime, the young ones are starting to go out through the inlets, some stay there all year round…" – Participant 10, 06 February 2019, p. 45, QIA 2019.

Pups are weaned after a six-week lactation period (Hammill et al. 1991). Mating occurs in the water underneath the ice around the time pups are weaned, during periods when females temporarily leave their den and enter the water (Lydersen 1995; Smith 1987). If mating is successful, this is the time when the egg becomes fertilized. Ringed seals have a gestation of 10–11 months, which includes the 2–3 months of suspended development (Hammill and Smith 1989; McLaren 1958; Smith 1987).

The timing of ringed seal aerial surveys is selected to overlap with the peak basking period in late May to early June (Smith and Hammill 1981), when more ringed seals are available for detection on the ice, and before an influx of ringed seals from the pack ice, which generally occurs in the later part of June (Smith and Hammill 1981). In June, during the peak basking period, ringed seals spend over 60% of the time on the ice (Kelly et al. 2010). Born et al. (2002) found the haul-out activity peaks in late June when ringed seals spend about 57% of the time hauled out. By July, the time out of the water drops to 30% as basking is completed and the foraging period begins (Kelly et al. 2010). Hunters in Arctic Bay use hunting methods to stalk basking and moulting seals in late spring, when ringed seals are hauled out at breathing holes, leads and ice edges (McLaren 1958; Smith 1973b; Finley 1979 in Furgal et al. 2002).

IQ reported in JCPS (2017) and QIA (2019) indicated springtime as the peak basking period for ringed seals:

"Seal harvesting occurs throughout Eclipse Sound at breathing holes, while seals are basking on the ice, and in leads, although not regularly during Upirngaaq (Arctic spring, roughly June)*"* – General Summary of workshop responses, p.29, JSPC 2017.

"I would catch enough to cache [hunted seal or narwhal] *for the winter. It would mainly be in the spring as this area is teeming with seals basking in the sun during springtime. There would be enough seal here to cache for the winter."* – Ipeelie Koonoo of Arctic Bay, as reported in Baffinland Iron Ore Corporation (2012, p. 25), p.29, QIA 2019.

1.4.1 Previous Ringed Seal Surveys in RSA

Ringed seal aerial surveys were first flown in Foxe Basin during June 2006, 2007, and 2008 to characterize baseline conditions (animal density and distribution) in the Southern RSA in support of the Final Environmental Impact Statement (FEIS; Baffinland 2012). Timing of the surveys corresponded with the basking/moulting period (late spring) when ringed seals spend the majority of their time on the sea ice and are therefore readily detectable and available for enumeration using aerial survey methods (Baffinland 2012). Visual observer data using strip-transect methods were analyzed for these surveys.

Survey design and monitoring methods differed between survey years. In 2007 and 2008, parallel east-west transects spaced nominally at 4-km intervals were surveyed to provide 25% coverage of the area. In 2006, parallel east-west transects were spaced farther apart at 10-km intervals compared to the nominal 4-km inter-transect spacing applied in 2007 and 2008. In 2006 and 2007, surveys were conducted from a fixed-wing aircraft (Dornier 228) and a helicopter (Eurocopter A Star), at an altitude of 150 m above sea level (asl) and a ground speed of 315 km/h (in 2006) and 220 km/h (in 2007). In 2008, surveys were conducted from a fixed-wing Twin Otter (DHC-6) aircraft at an altitude of 91 m asl and at a ground speed of 220 km/h.

Ringed seal density in Steensby Inlet was estimated at 0.20 seals/km^2 in 2006, 1.57 seals/km^2 in 2007 and 0.71 seals/km^2 in 2008 (Baffinland 2012). Ringed seal density in Tasiujaq (formerly known as Murray Maxwell Bay) was estimated at 1.26 seals/km^2 in 2008 (Baffinland 2012).

2.0 METHODS

2.1 Study Area and Design

The 2021 aerial survey was conducted over a single day on 13 June. The 2024 aerial survey was conducted from 7 to 12 June. In both survey years, the survey team was comprised of two pilots and two marine mammal biologists (one WSP employee and one contractor) both with prior marine mammal survey experience in the Eastern Canadian Arctic. One Inuit researcher from Arctic Bay participated in the 2024 survey. No Inuit researchers participated in the 2021 survey due to COVID-19 restrictions in Nunavut at this time.

The study area for the RSASP was delineated based on spatial boundaries established in the FEIS (Baffinland 2012), with Tasiujaq selected as a control area based on its general proximity to the proposed port facility while still remaining physical isolated from the planned Project activities. Aerial surveys were implemented to assess the distribution and density of ringed seals in the RSA during the peak moulting period, specifically when individuals remain hauled out on the sea ice in high numbers. The aerial survey program targeted two separate areas (i.e., strata) of winter landfast ice in the RSA: Steensby Inlet where the proposed port facility will be situated, and Tasiujaq, designated as an adjacent control area (see Figure 2).

Survey design and data collection methods were based on Young et al. (2019), employing strip-transect analysis of infrared imagery in combination with high-resolution digital photography. The 2021 and 2024 survey platform consisted of a de Havilland Twin Otter (DHC-6) fixed-wing aircraft, equipped with a ventral camera port. Systematic line-transect surveys were flown in both strata when conditions allowed, with the location of the first transect line randomly selected. Transects were evenly distributed across the survey area at an inter-transect distance of ~4-km (Figure 2). In the Steensby Inlet stratum, twenty-four transects (green in Figure 2) were oriented in an east-west parallel line direction. In the Tasiujaq stratum, twenty-two transects (yellow in Figure 2) were oriented in a north-south parallel line direction.

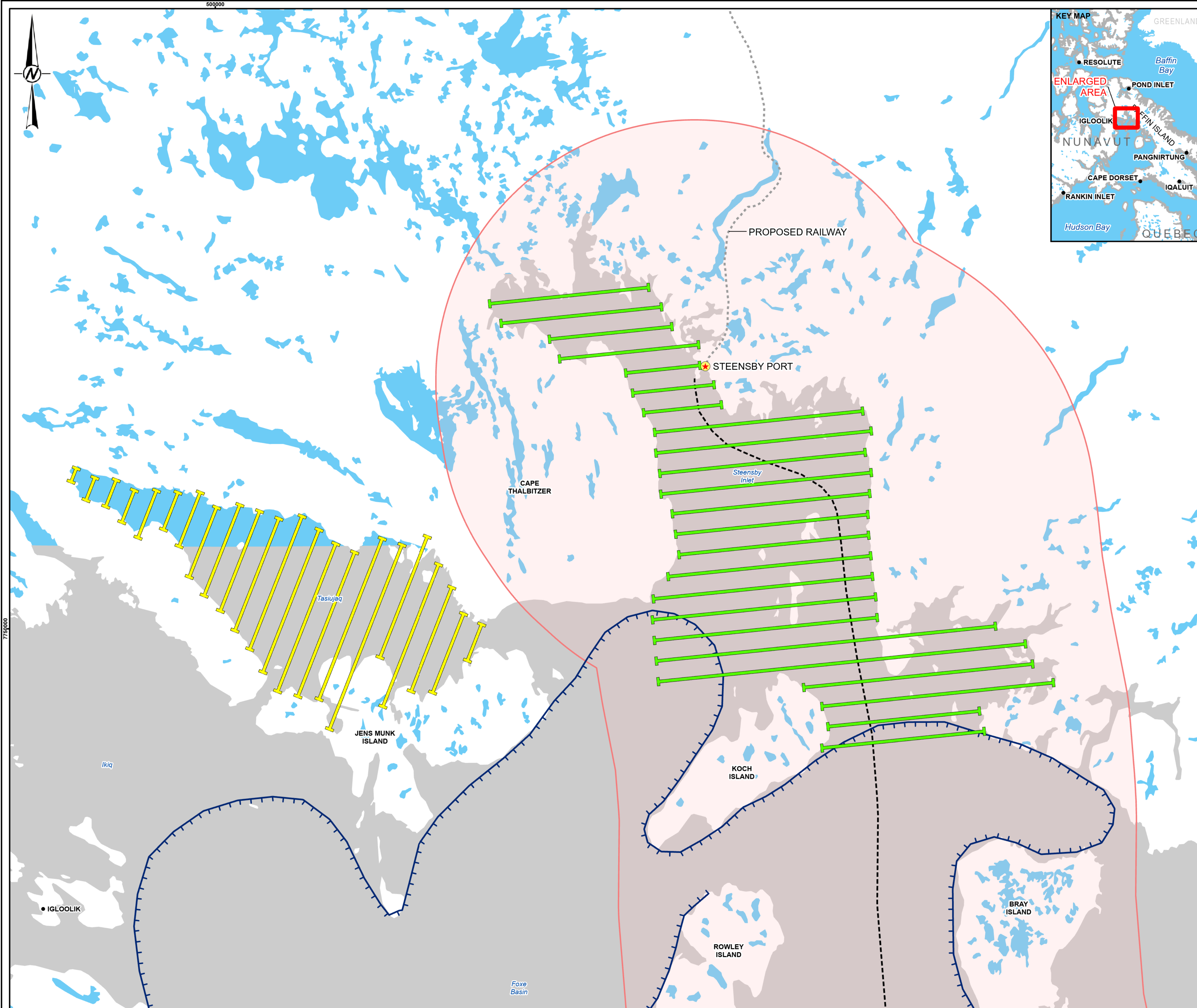

LEGEND

- COMMUNITY
- PORT LOCATION
- FLOE EDGE - IQ (BAFFINLAND 2012B,F)
- PROPOSED RAILWAY
- SHIPPING ROUTE (APPROXIMATE)
- LOCAL STUDY AREA
- MARINE REGIONAL STUDY AREA
- WATERBODY

RINGED SEAL SURVEY TRANSECTS

- STEENSBY INLET
- TASIUJAQ

0 25 50

1:750,000 KILOMETRES

REFERENCE(S)

BASE DATA OBTAINED FROM GEOGRATIS, © DEPARTMENT OF NATURAL RESOURCES CANADA. ALL RIGHTS RESERVED. SHIPPING ROUTE PROVIDED BY CLIENT, JUNE 8, 2022. NUNAVUT SETTLEMENT BOUNDARY OBTAINED FROM NUNAVUT TUNNGAVIK INC., OCTOBER 9, 2012. PROJECTED COORDINATE SYSTEM: NAD 1983 UTM ZONE 17N

CLIENT
BAFFINLAND IRON MINES CORPORATION

PROJECT
MARY RIVER PROJECT
2021 & 2024 RINGED SEAL AERIAL SURVEYS

TITLE
TRANSECTS FOR 2021 AND 2024 RINGED SEAL AERIAL SURVEYS IN STEENSBY INLET AND TASIUJAQ

CONSULTANT
wsp

YYYY-MM-DD	2025-10-28
DESIGNED	TT
PREPARED	AA
REVIEWED	TT
APPROVED	PA

PROJECT NO.	CONTROL	REV.	FIGURE
CA0051512.6683	1000.01	0	2

IF THIS MEASUREMENT DOES NOT MATCH WHAT IS SHOWN, THE SHEET SIZE HAS BEEN MODIFIED FROM: ANSI B

2.2 Data Collection

Data collection utilised strip-transect methods combining infrared imagery and digital photographs, as described in Young et al. (2019). Transects were flown at a ground speed of 204 km/hour (110 knots) at an altitude of 305 m (1,000 ft) asl. Aircraft location, position, altitude, speed, and heading were recorded every second using a Bluetooth global positioning system (GPS) unit and iPad, along with navigational mapping software (Foreflight), which was programmed with the survey transect grid.

A dedicated data recorder entered environmental conditions into Mysticetus™ software at the beginning and end of each transect, and when changes in survey conditions occurred along an active transect. Environmental survey condition categories included cloud cover (percent), surface air temperature (°C), surface wind speed (km/h), surface wind direction (N, S, E, W), ice cover (in tenths), ice type, snow/ice roughness (percent), fog cover (in tenths), and fog intensity. Air temperature and wind variables were obtained from Windy.com, specifically using the ECMWF (European Centre for Medium-Range Weather Forecasts) model of surface conditions either during or immediately after the flight (depending on network coverage). Snow/ice roughness was subjectively estimated based on the percent of snow drift or ice ridges that covered the surface of the ice (i.e., 0% snow/ice roughness represents a smooth ice surface with no snow drifts or ice ridges, whereas a 50% roughness represents an ice surface with 50% of it covered in snow drifts and/or ice ridges).

Thermal infrared imagery was obtained using a forward-looking infrared camera (FLIR T1020) with a 45° lens. At the target altitude of 305 m, the strip width covered by the FLIR imagery was approximately 250 m wide strip directly below the aircraft. The FLIR T1020 used an uncooled microbolometer-type sensor with a resolution of 1,024 x 768 pixels and detected infrared radiation in the range of 7.5–14 μm. The FLIR camera was connected to a laptop and controlled remotely by a camera operator using FLIR ResearchIR Max software version 4.40.11.35 (FLIR Systems, Inc., Wilsonville, OR, USA).

In 2021, visible light (visual) photographs were obtained using a Canon EOS 5DS R DSLR (digital single-lens reflex) camera fitted with a 35 mm lens (Sigma 35 mm f/1.4 DG HSM). Visual photographs were taken at an interval of two seconds, providing approximately 50% overlap between consecutive photos. At the target altitude of 305 m, the strip width covered by the DSLR camera was 313 m focused directly below the aircraft. Photographs taken with the DSLR camera were captured in .jpg format at the maximum camera resolution setting of 8,688 x 5,792 pixels. The camera was connected to a laptop and controlled remotely by an operator using Breeze Multi-Camera Array software version v2.1.2 (Breeze Systems Limited, Camberley, Surrey, UK).

In 2024, visible light (visual) photographs were obtained using a FujiFilm GFX 100S medium format mirrorless camera fitted with a 45 mm lens (Fujifilm 45 mm f/2.8 WR). Visual photographs were taken at an interval of three seconds (using an intervalometer), providing approximately 30% overlap between consecutive photos. At the target altitude of 305 m, the strip width covered by the DSLR camera was 297 m wide strip directly below the aircraft. Visual photographs taken with the FujiFilm GFX 100S were captured in .jpg format at the maximum camera resolution setting of 11,648 x 8,736 pixels.

2.3 Data Analysis

2.3.1 Strip-Transect Analysis for Densities

A single analyst from a third-party contractor (Whale Seeker Inc.) analyzed the infrared video files using FLIR ResearchIR Max software version 4.40.11.35 (FLIR Systems, Inc., Wilsonville, OR, USA). This software allowed the user to view FLIR infrared video files and provided tools to visually identify temperature spikes indicative of potential seals.

All potential seals observed in the infrared imagery were verified by viewing the corresponding visual images obtained from the DSLR camera (Figure 3). Through this verification process, only visual photographs that corresponded to potential seals in the infrared imagery were included in the analysis.

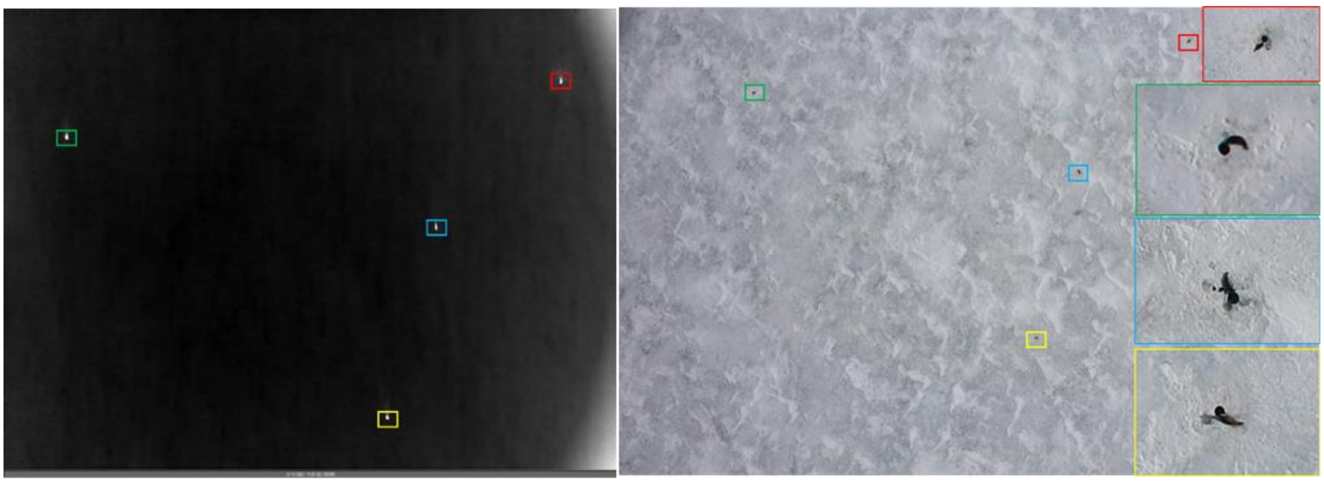

Figure 3: Example of paired aerial images from infrared camera (left) and DSLR camera (right) collected during the 2021 RSASP demonstrating infrared imagery with visual photographs. Insert images show close-up views of seals in the visual photographs.

To assess the success rate of the infrared camera, an experienced observer analyzed a random set of 1,463 visual photographs from the dataset. Seals identified in the visual photographs were compared with the results of the infrared imagery analysis to determine whether the infrared method was missing (i.e., failed detection of) seals that were detected in the visual photographs.

Strip-transect analysis was performed on “infrared” data obtained from infrared imagery within a 250 m wide strip following the methods of Young et al. (2015) and Chambellant et al. (2012b). The perpendicular distance of the sighting from the track line was retrieved from the pixel position of the sighting on the photographs. Sightings beyond 125 m from the track line were excluded from the analysis. The density of hauled-out ringed seals per km^2 was estimated following Buckland et al. (2001) by computing the number of detected seals over the surveyed strip area:

$$\hat{D} = \sum_{i=1}^{k} n_i / \omega \sum_{i=1}^{k} l_i$$

where k is the number of transects flown, n_i is the number of ringed seals counted on the i^{th} transect, ω is the width of the strip, and l_i is the length of the i^{th} transect.

Following Kingsley and Smith (1981), the variance of density was determined by:

$$\sigma^2(\hat{D}) = k \times \frac{\sum_{i=1}^{k-1}(d_i - d_{i+1})^2}{2(k-1) \times (\omega \sum_{i=1}^{k} l_i)^2}$$

where

$$d_i = n_i - \hat{D} \times \omega l_i$$

The coefficient of variation (CV) of the estimated density was calculated by dividing the square root of the variance by the estimated density.

Densities calculated in this report are not corrected for availability bias (proportion of seals not hauled out and not visible to be counted) and should be considered indices and not absolute estimates.

2.3.2 Univariate Analyses

The χ^2 (chi-square) goodness-of-fit test was used to compare sightings of ringed seals in different habitat, weather, and time-of-day categories collected during the surveys. Observed ringed seal sightings were based on a transect strip of 125 m in width on each side of the aircraft. Variables included time of day, date, air temperature, wind speed, and cloud cover. Strata with relatively small surveyed areas (<10 km^2) are excluded from analyses. Although statistical tests were always based on seal sightings, results were discussed in terms of observed seal densities (seals/km^2).

2.3.3 Density Surface Modelling for Hotspots

A density surface modelling (DSM) framework was used to model spatially-referenced count data with the additional environmental data and distances collected to account for imperfect detection. Modelling proceeded in two steps. First, a multiple covariate distance sampling (MCDS) detection function was fitted to the perpendicular distance data to obtain detection probabilities for individuals. Second, counts were then summarised per segment (contiguous transect sections), and a generalized additive model (GAM, Wood 2006) was then constructed with the per-segment counts as the response. GAMs provided a flexible class of models that included generalized linear models but extended them with the possible addition of splines to create smooth functions of covariates. DSM modelling was performed within the R software environment (v4.5.1; R Core Team 2025) using the dsm, mgcv and Distance packages (Miller et al. 2021; Wood 2021; Miller 2021). The geographic and temporal separation between the Tasiujaq and Steensby study areas and years of surveying (2021 and 2024) required the fitting of at least four separate global models (two for each study area).

Ideally, the maximum segment length is such that neither the density of objects nor the covariate values varies appreciably within segments. Initially, a 100 m by 100 m resolution bathymetry dataset was implemented (IBCAO v5, 2024). It was discounted due to issues with the inclusion of radar altimetry data that grossly inflated elevations in some shallow ocean areas. A 200 m by 200 m resolution bathymetry dataset (IBCAO v4, 2020) with more precise bathymetry in shallow areas was ultimately used. It should be noted that bathymetry in the Steensby/Tasiujaq area is largely interpolated from sparse data points. The detailed bathymetry available for the approach to the Steensby Port facility was not included since it only covered a small portion of the Steensby study area and none of the Tasiujaq study area. This limited distribution of detailed bathymetry would result in biases toward the survey data in the detailed bathymetry area. The inclusion of a tidal dataset was intended, but the available products had low spatial resolution and simplified coastal geography that would not correlate well with the detailed coastline information used in this study.

For each ~1km segment, the following multiple static environmental covariates were extracted: latitude, longitude, distance from the nearest shore, mean depth, mean slope, and distance from floe edge. Additional segment covariates of maximum and minimum depth were also extracted from the bathymetry. The segment centroid was used for determining latitude, longitude and distance calculations, while bathymetry data was extracted from a 125 m buffer on the transect segment to capture bathymetry data points (model truncation distance). The manipulation and measurement of spatial data was performed with ESRI ArcMap 10.8.2 ArcInfo license with the Spatial Analyst toolbox (ESRI 2021). A Lambert conformal conic projection, with origin centred on the project area, was used to ensure that distance measurements were uniform across the study area. Floe edge locations were estimated using satellite imagery (Zoom Earth 2025) and digitized for inclusion in the spatial data. The floe edges did not noticeably change during the survey period within a survey year. Since two complete surveys were completed in 2024, the survey number was included as a factor covariate for the 2024 surveys. Count per segment was then modelled as a sum of smooth functions of covariates (e.g., location, depth, distance to shore, measured at the segment level) using a GAM. Smooth functions were modelled as splines, providing flexible curves and surfaces to describe the relationship between the covariates and the response.

To predict across the study areas with the fitted model, a 1 km^2 prediction grid was created in ArcMap, and the cells were clipped to the coastline and floe edges. Grid cell areas were calculated to be used as the offset value during prediction. Environmental covariates were extracted using the same methodology as was completed for the segments.

<u>Detection Function</u>

The DSM methodology involved two separate statistical models. The first statistical model was a fitted detection function to the perpendicular sighting distances, as in a conventional distance-sampling analysis, to estimate the detection probability. Normally, this model compensates for observer bias, but this isn’t expected to be an issue with imagery data. Alternatively, this model is used to compensate for availability bias, whereby the species of interest changes its surface availability depending on environmental covariates. The expectation is that ringed seals will dive depending on the proximity of the aircraft and will vary the distance at which they dive depending on covariates that could alter their ability to detect the aircraft. Environmental variables that may affect the seal’s ability to detect the aircraft (wind speed, aircraft travel direction and travel direction relative to wind direction) were incorporated as covariates (Marques et al. 2007). The best detection function model was selected based on Akaike’s Information Criterion (AIC) values. When the probability of detection (p) was high ($p > 0.98$), the detection function was considered unnecessary due to the minimal correction it would provide.

Spatial Model Fitting

The second statistical model was a spatial density component. The abundance of ringed seals seen in each segment was described by a GAM via a Horvitz-Thompson estimator with segment effort indicated by the area of each segment (length by a width twice that of the detection function truncation distance). Problems can occur when smoothing over areas with complicated geography using a standard xy smoother (e.g., peninsulas or islands), where the proximity of counts on one side of a feature would unrealistically influence the model's interpretation of counts on the other side of the feature. Therefore, we also attempted to fit a "soap film" smoother (Wood et al. 2008) to the spatial data, which usually performs better for complex study regions by reducing the smoothing of density contours across land boundaries and minimizing edge effects. The soap film is a bivariate smooth of spatial coordinates that requires a grid of "soap knots" within the study area. Various densities of "soap knots" are trialled to assess the performance of the smoother and assess over-fitting of the data. Over-fitting the soap film smoother can result in unrealistic hotspots and account for more of the variance in the data that could otherwise have been accounted for by environmental covariates.

All potential model covariates (including x and y coordinates) were tested for collinearity using R tools provided by Highland Statistics Ltd. (Zuur et al. 2009). As expected, maximum, minimum and mean depth were collinear and could only be run individually in a model. Distance to floe edge was sometimes problematic with collinearity with the x or y coordinates. The four global models were run with all possible covariate groupings, dependent on collinearity constraints. Alternate variables were swapped out and run separately when appropriate. Models excluding a spatial component were also run. These global models were also run separately for each distribution family. The relative magnitudes of each smoother's basis size (k) and its resulting effective degrees of freedom (edf) value were examined for the presence of unrealistically high values that could indicate over-fitting, and to also ensure that smooth functions were given sufficient freedom to describe the underlying covariate relationship (k was then adjusted accordingly as necessary). Smoothing parameter estimates were optimized using restricted maximum likelihood (REML). To address zero-inflation, which is a common cause of overdispersion in count data, candidate models were fit with negative binomial or Tweedie response distributions in addition to the Poisson distribution.

Model Selection and Validation

For each response distribution family, AIC values were used to select the best-fit models from the candidates. The top candidate models from the different response distributions were then assessed using quantile-quantile (QQ) plots that included reference bands produced by repeated simulations of new response data from the fitted model. Departure of the residuals from the bounds of the reference bands indicates a misspecification of the model (see Augustin et al. 2012) and thus can be used to assess fit and eliminate a model from the candidate set (i.e. incorrect distribution family used). Model fit was also checked using the 'DHARMa' package (Hartig 2020) in R, while model residuals were also tested for spatial autocorrelation using Moran's I test via the DHARMa package.

It was assumed that the modelled detection function was independent of the GAM, with the total variance of the abundance estimated using the delta method (Seber 1982) to combine the detection model and spatial component variances (Hedley & Buckland 2004).

2.3.3.1 Hotspot Analysis

We used a spatial statistical approach (Getis-Ord Gi*) with two types of neighborhood definitions to identify hotspots. The Gi* method identifies spatial clusters of high or low density (individuals per km²), where these clusters differ from patterns expected under random spatial processes. Gi* follows the basic form:

$$G_i^*(d) = \frac{\sum_j \omega_{(ij)(d)x_j}}{\sum_{j=1}^{n} x_j}$$

where i is the pivot location, x is the attribute value of i—in this case, density—and ω_{ij} is a spatial weights matrix created using a distance threshold (d) or the spatial configuration of adjacent cells to define neighbors of the ith observation (Getis and Ord 1992; Ord and Getis 1995). Hotspots are determined when a pivot location and its surrounding neighborhood, defined by ω_{ij}, exhibit high density values (individuals per km²) relative to all density measurements within the study area. Permutation testing was employed to assess whether the observed clustering deviates from expectations based on randomly generated patterns. The Gi* statistic was calculated using GeoDa software (v.1.6.6, October 2014; Anselin et al., 2010) with 999 permutations to establish statistical significance at the 0.05 level.

Spatial neighborhoods (ω_{ij}) can be defined in several ways, and the chosen method will impact which locations are identified as hotspots. In this study, we utilized contiguity-based neighborhood definitions, a standard approach for areal datasets (Dubin 2009). Contiguity matrices are typically used to analyze adjacency relationships among areal units. For ecological research, equal area grids are often employed to represent continuous phenomena (Birch et al. 2007), naturally lending themselves to contiguity definitions. We incorporated first-order contiguity; first-order neighborhoods include cells sharing a direct boundary with the focal cell (lag 1; Nelson and Robertson 2012). Adjacency is characterized using chess piece movements—rook, bishop, and queen (Dubin 2009). This analysis applied queen contiguity, which encompasses any neighboring cell that shares a border with the focal cell, irrespective of orientation.

3.0 RESULTS

3.1 Ice Coverage

Landfast ice conditions observed during the 2021 (Figure 4) and 2024 (Figure 5) ringed seal aerial surveys in Steensby Inlet demonstrated variability in both extent and melt progression. In 2024, landfast ice covered a larger area of Steensby Inlet (3,318 km²) relative to 2021 (3,196 km²), attributable to shifts in the position of the floe edge. By 13 June 2021, landfast ice within the Steensby Inlet region had reached an advanced melt stage, as indicated by widespread exposed blue ice following snowmelt (Figure 4). Conversely, comparable ice conditions were not present until 17 June 2024, suggesting that the melt progression in 2024 lagged approximately four days behind that of 2021.

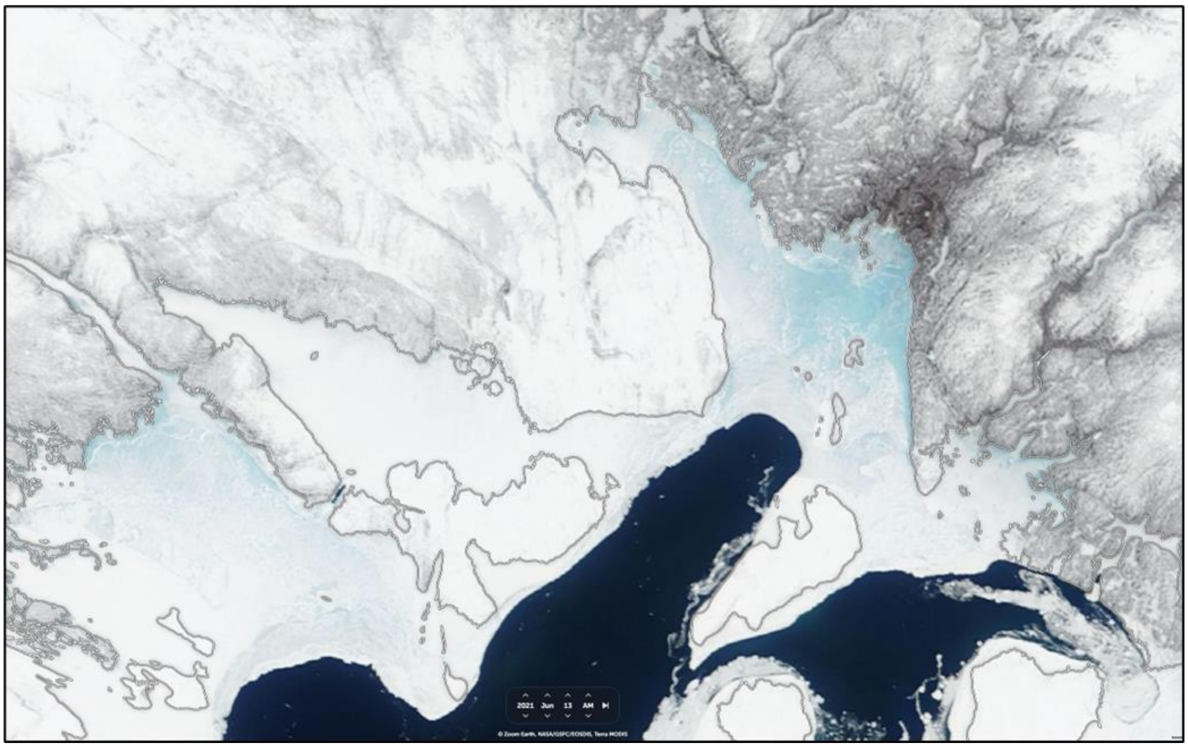

Figure 4: Satellite image on 13 June 2021 (Zoom Earth; https://zoom.earth) showing ice conditions in Steensby Inlet and Tasiujaq area during the 2021 aerial surveys.

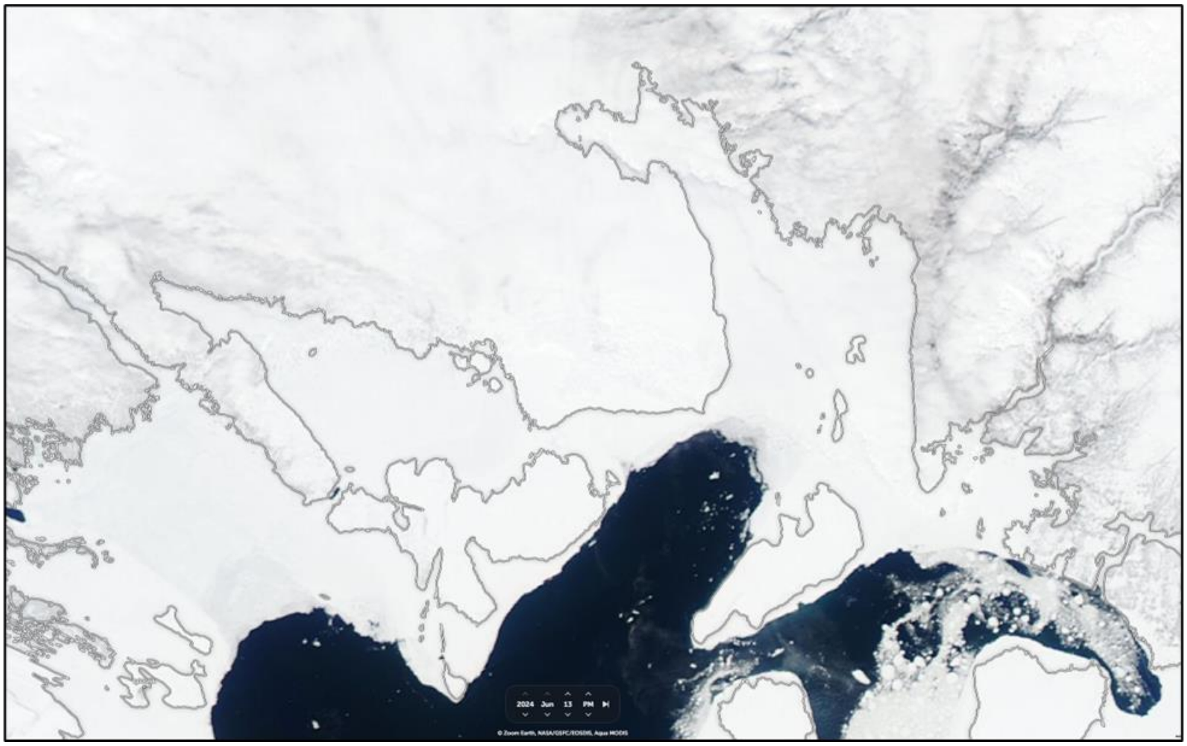

Figure 5: Satellite image on 13 June 2024 (Zoom Earth; https://zoom.earth) showing ice conditions in Steensby Inlet and Tasiujaq area during the 2024 aerial surveys.

3.2 Survey Coverage

One survey was completed on 13 June 2021, and two surveys were completed between 7–12 June 2024 (Table 1). Over the course of the three surveys, a total of 3,428.7 km of survey effort was conducted. All survey effort was flown over 10/10 landfast ice coverage. Surveys were flown between 07:30 and 18:30, whenever weather conditions allowed.

Table 1: Survey effort for 2021 and 2024 ringed seal aerial surveys.

Date	Survey #	Strata	Effort (km)
13 June 2021	1	Steensby Inlet	730.3
13 June 2021	1	Tasiujaq	380.5
Subtotal	1	—	1,110.8
7 & 8 June 2024	2	Steensby Inlet	773.1
8 June 2024	2	Tasiujaq	388.4
Subtotal	2	—	1,161.5
9 & 12 June 2024	3	Steensby Inlet	789.9
12 June 2024	3	Tasiujaq	366.5
Subtotal	3	—	1,156.4

3.3 Sighting Conditions

An observer onboard the aircraft recorded environmental and sighting conditions at the beginning and end of each transect and when conditions changed along the transect/flight path.

Cloud Cover

Cloud cover during the 2021 and 2024 RSASP ranged from 0 to 100%. In 2021, during Survey 1, 100% of the survey effort was flown in 0% cloud cover (Figure 6). In 2024, during Survey 2, over 70% of the survey effort was flown in 0% cloud cover in Steensby Inlet, whereas cloud cover in Tasiujaq varied between 0-90% (Figure 6). During Survey 3, 99% of the survey effort was flown in 100% cloud cover (Figure 6).

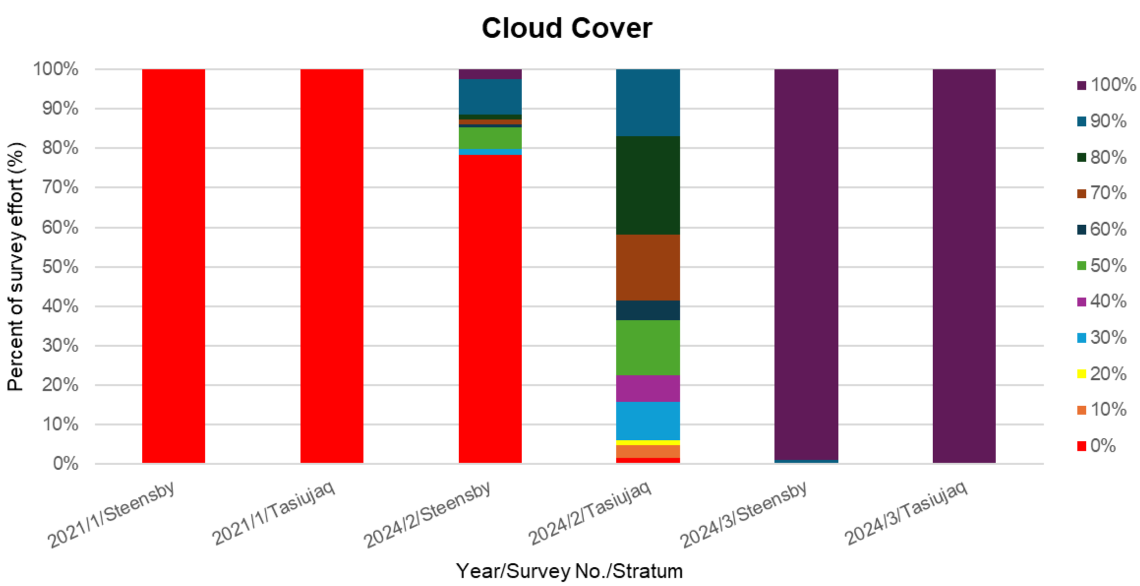

Figure 6: Proportional breakdown of cloud cover during 2021 and 2024 RSASP.

Air Temperature

Ground air temperatures during the 2021 and 2024 RSASP ranged from -2°C to 4°C (Figure 7). In 2021, during Survey 1, conditions ranged from 2°C to 4°C with a mean air temperature of 2.9°C. In 2024, air temperatures were colder than in 2021. Survey 2 air temperature ranged from -1°C to 2°C with a mean of -0.1°C. During Survey 3, air temperature ranged from -2°C to 1°C with a mean of -0.2°C.

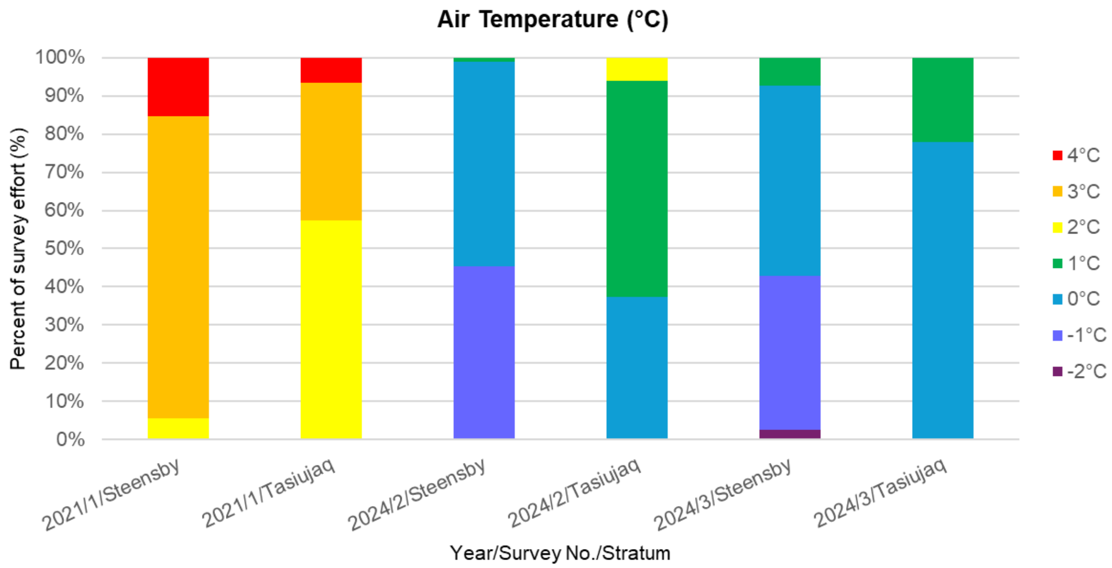

Figure 7: Proportional breakdown of air temperature during 2021 and 2024 RSASP.

Wind Speed

Ground wind speeds ranged from 0 to 22 km/h during the 2021 and 2024 RSASP. In 2021, during Survey 1, wind speeds ranged from 5 to 22 km/h with a mean of 12.8 km/h. The majority (69%) of the survey effort flown during Survey 1 was with wind speeds ranging from 0 to 15 km/h (Figure 8). In 2024, wind speed during Survey 2 ranged from 2 to 18 km/h with a mean of 10.2 km/h. The majority (86%) of the survey effort flown during Survey 2 was with wind speeds ranging from 0 to 15 km/h (Figure 8). During Survey 3, wind speed ranged from 1 to 15 km/h with a mean of 8.4 km/h (Figure 8).

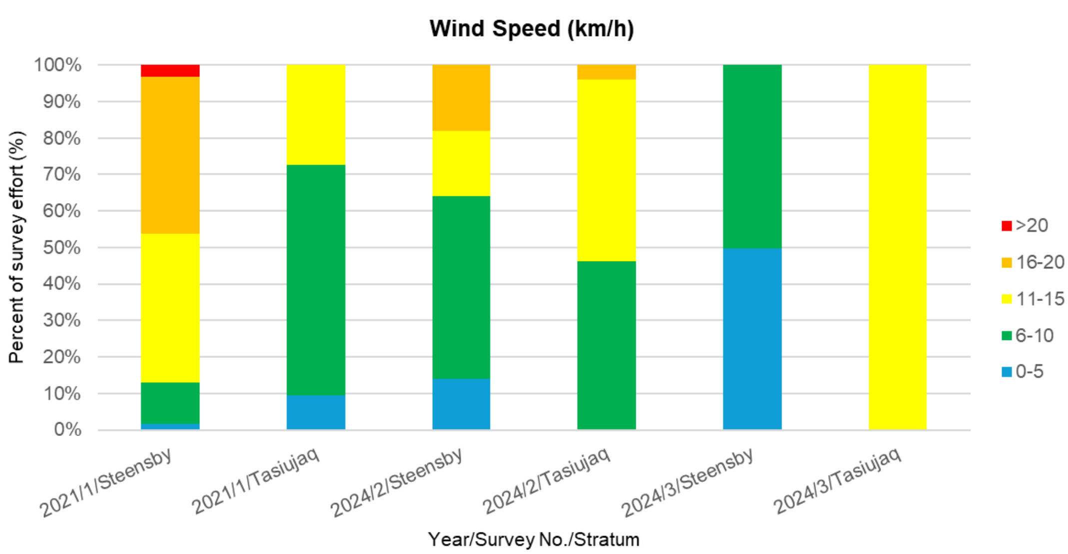

Figure 8: Proportional breakdown of wind speed during the 2021 and 2024 RSASP.

Wind Direction

Wind direction varied during the 2021 and 2024 RSASP due to the large study area. During Surveys 1 and 2, the majority (100% and 96%, respectively) of the survey effort was flown in areas with northerly wind directions (NW, N, and NE; Figure 9). During Survey 3, 53% of the survey effort was flown in areas with northerly wind directions (NW, N, and NE; Figure 9). Wind direction was more variable during Survey 3.

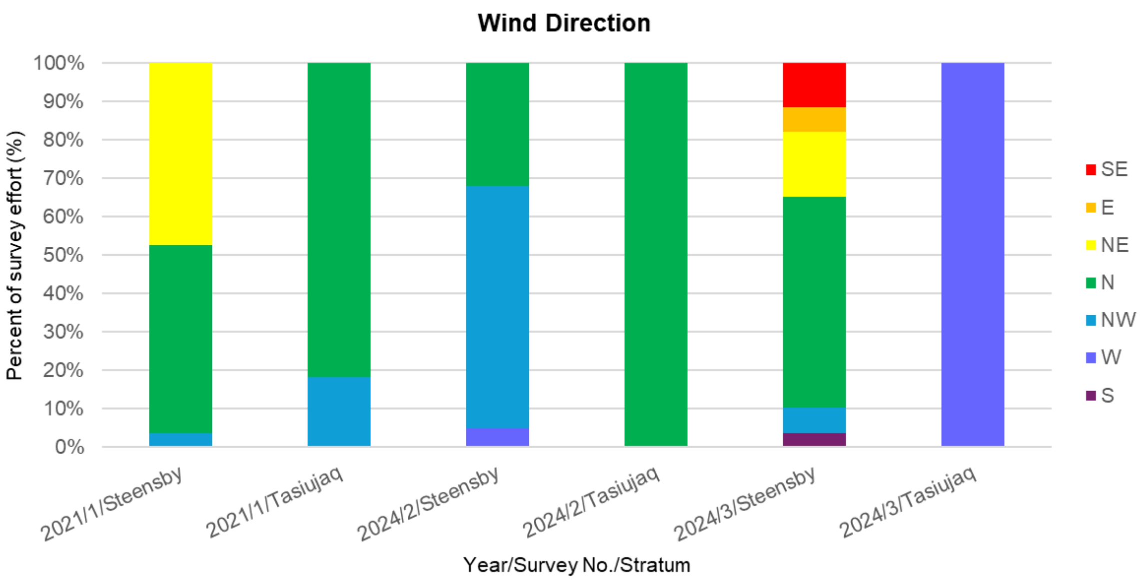

Figure 9: Proportional breakdown of wind direction during the 2021 and 2024 RSASP.

Snow/Ice Roughness

Snow/ice roughness during the 2021 and 2024 RSASP ranged from 0 to 90%. A 0% roughness represents a smooth ice surface with no snow drifts or ice ridges, whereas a 50% roughness represents an ice surface with 50% of it covered in snow drifts and/or ice ridges. During Survey 1, conditions ranged from 0% to 80% snow/ice roughness, with the majority (91%) of the survey effort flown in 0% to 30% snow/ice roughness (Figure 10). During Survey 2, conditions ranged from 10% to 90% snow/ice roughness, with the majority (95%) of the survey effort flown in 10% to 30% snow/ice roughness (Figure 10). During Survey 3, conditions ranged from 10% to 60% snow/ice roughness, with the majority (96%) of the survey effort flown in 10% to 30% snow/ice roughness (Figure 10).

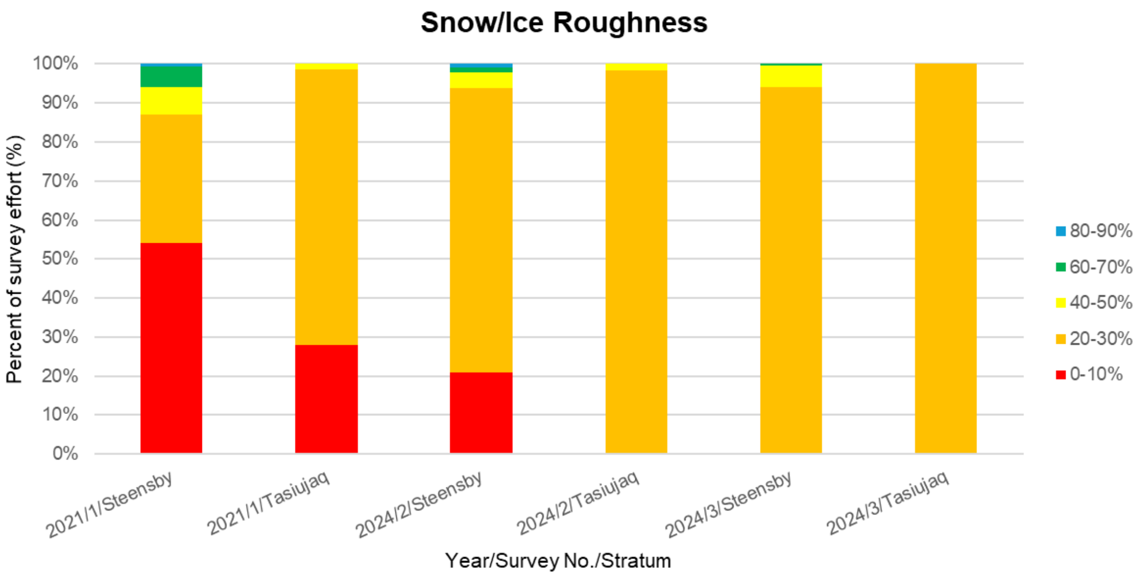

Figure 10: Proportional breakdown of snow/ice roughness during the 2021 and 2024 RSASP.

3.4 Survey Sightings

A total of 746 potential animal observations were identified during the analysis of the infrared imagery. Of these potential observations, 561 (75%) were confirmed to be animals, while 185 (25%) were identified as warmer areas on the ice created by a combination of melt ponds, rocks, dirt, debris, or garbage. Figure 3 shows how infrared imagery matches up with the digital photographs for confirming observations. The 561 confirmed marine mammal observations consisted of 557 ringed seal observations and four polar bears observed both on and off the transect.

Ringed seals were observed throughout the survey area during the three surveys (Figures 11–13). Ringed seal group sizes ranged from single animals to a group size of four, with mean and median group sizes of 1.1 and 1.0, respectively. Fourteen ringed seal pups were observed during the surveys.

In the analysis of a random set of 1,463 visual photographs to assess the success rate of the infrared camera data, 16 ringed seal observations were detected in both the infrared method and the independent analysis of the visual photographs, two seal observations were detected in the infrared method but missed in the independent analysis of the visual photographs, and three seal observations were detected in the independent analysis of the visual photographs but missed in the infrared method. The three seal observations that were missed in the infrared method were outside of the field of view (250 m) of the FLIR and thus expected to be missed and would not have been captured in the data analysis. Of the 18 seal observations within the FLIR field of view, the infrared method was 100% effective in detecting seal observations (18 out of 18 available sightings), and the independent analysis of the visual photographs was 89% effective in detecting seal observations (16 out of 18 available sightings).

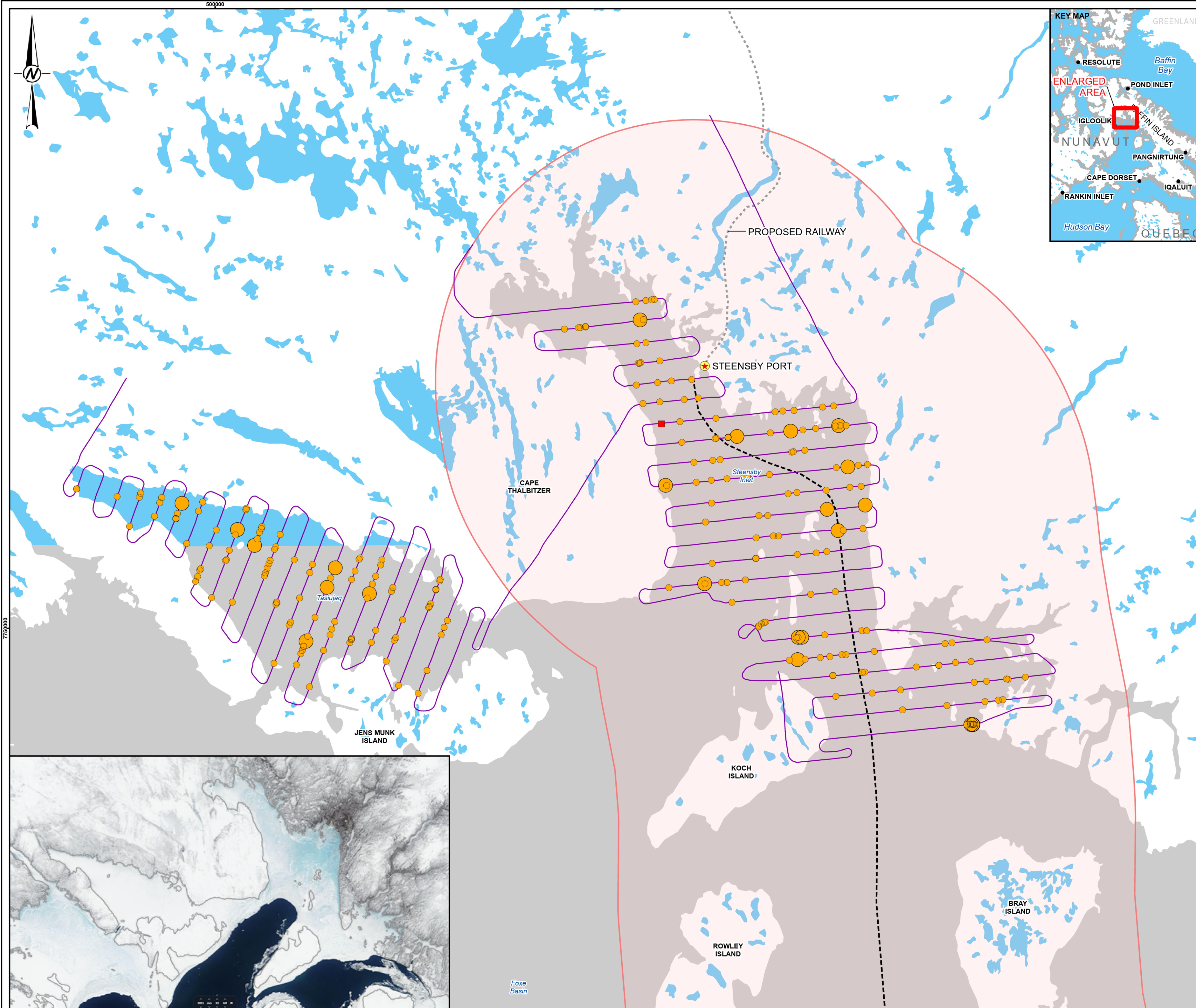

LEGEND

- COMMUNITY
- PORT LOCATION
- PROPOSED RAILWAY
- SHIPPING ROUTE (APPROXIMATE)
- SURVEY TRACK
- LOCAL STUDY AREA
- MARINE REGIONAL STUDY AREA
- WATERBODY

MARINE MAMMAL SPECIES OBSERVATIONS (GROUP SIZE)

POLAR BEAR

- 1

RINGED SEAL

- 1
- 2-4

0 25 50
1:750,000 KILOMETRES

REFERENCE(S)

BASE DATA OBTAINED FROM GEOGRATIS, © DEPARTMENT OF NATURAL RESOURCES CANADA. ALL RIGHTS RESERVED. SHIPPING ROUTE PROVIDED BY CLIENT, JUNE 8, 2022. NUNAVUT SETTLEMENT BOUNDARY OBTAINED FROM NUNAVUT TUNNGAVIK INC., OCTOBER 9, 2012. PROJECTED COORDINATE SYSTEM: NAD 1983 UTM ZONE 17N

CLIENT
BAFFINLAND IRON MINES CORPORATION

PROJECT
MARY RIVER PROJECT
2021 & 2024 RINGED SEAL AERIAL SURVEYS

TITLE
DISTRIBUTION OF RINGED SEALS AND POLAR BEARS RECORDED DURING AERIAL SURVEY ON 13 JUNE 2021

CONSULTANT

YYYY-MM-DD	2025-10-28
DESIGNED	TT
PREPARED	AA
REVIEWED	TT
APPROVED	PA

PROJECT NO.	CONTROL	REV.	FIGURE
CA0051512.6683	1000.01	0	11

IF THIS MEASUREMENT DOES NOT MATCH WHAT IS SHOWN, THE SHEET SIZE HAS BEEN MODIFIED FROM ANSI B
25mm

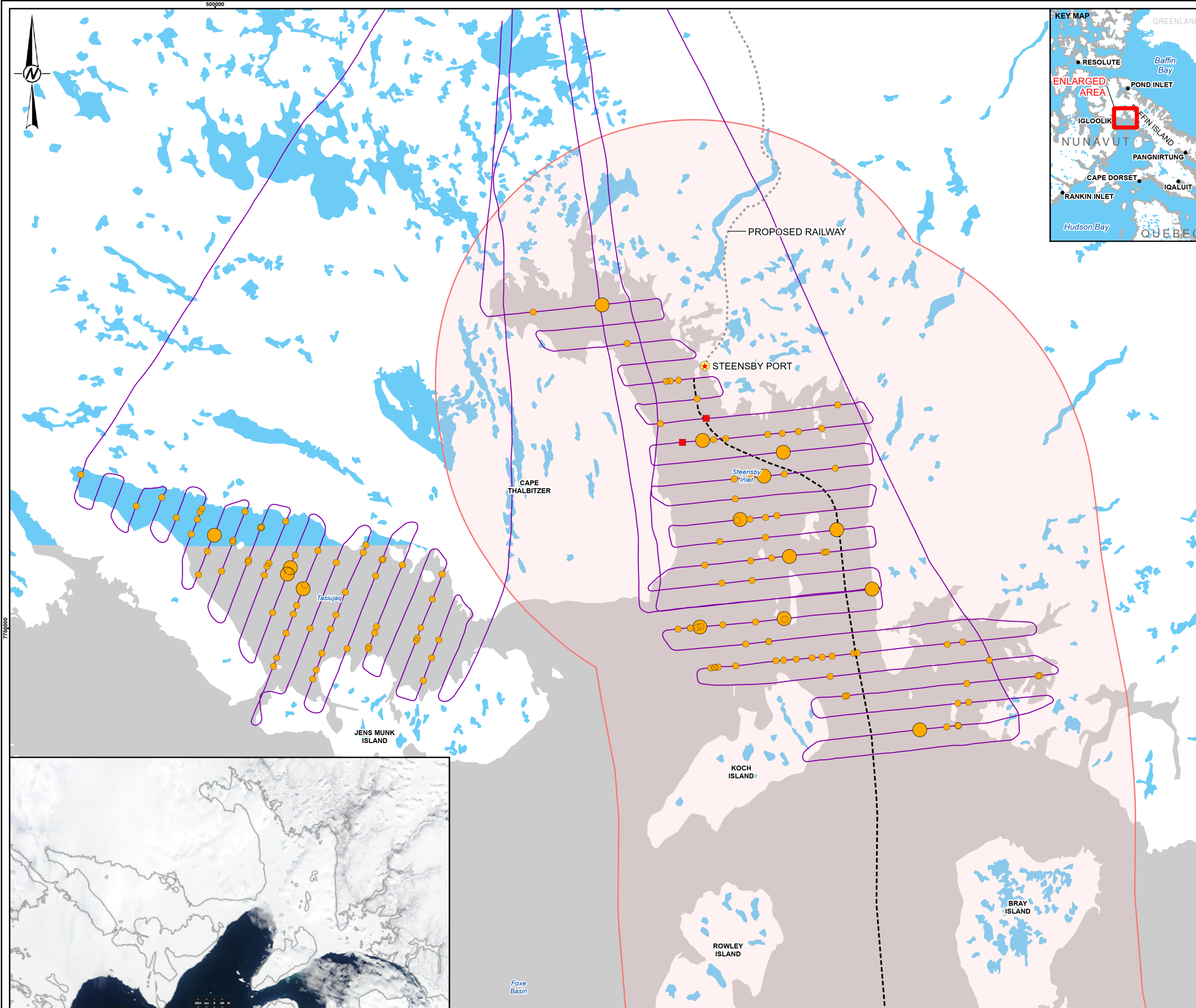

LEGEND

- COMMUNITY
- PORT LOCATION
- PROPOSED RAILWAY
- SHIPPING ROUTE (APPROXIMATE)
- SURVEY TRACK
- LOCAL STUDY AREA
- MARINE REGIONAL STUDY AREA
- WATERBODY

MARINE MAMMAL SPECIES OBSERVATIONS (GROUP SIZE)

POLAR BEAR

- 1

RINGED SEAL

- 1
- 2-4

0 25 50

1:750,000 KILOMETRES

REFERENCE(S)

BASE DATA OBTAINED FROM GEOGRATIS, © DEPARTMENT OF NATURAL RESOURCES CANADA. ALL RIGHTS RESERVED. SHIPPING ROUTE PROVIDED BY CLIENT, JUNE 8, 2022. NUNAVUT SETTLEMENT BOUNDARY OBTAINED FROM NUNAVUT TUNNGAVIK INC., OCTOBER 9, 2012. PROJECTED COORDINATE SYSTEM: NAD 1983 UTM ZONE 17N

CLIENT

BAFFINLAND IRON MINES CORPORATION

PROJECT

MARY RIVER PROJECT
2021 & 2024 RINGED SEAL AERIAL SURVEYS

TITLE

DISTRIBUTION OF RINGED SEALS AND POLAR BEARS RECORDED DURING AERIAL SURVEY ON 7-8 JUNE 2024

CONSULTANT

wsp

YYYY-MM-DD	2025-10-28
DESIGNED	TT
PREPARED	AA
REVIEWED	TT
APPROVED	PA

PROJECT NO.	CONTROL	REV.	FIGURE
CA0051512.6683	1000.01	0	12

PATH: I:\CLIENTS\BAFFINLAND_IRON_MINES\CA0051512_6683\Mapping\1000_RingedSealSurvey2024\CA0051512_6683_1000_Fig12_AerialSurvey_7_8Jun2024_Rev0.aprx PRINTED ON: AT: 12:59:32 PM

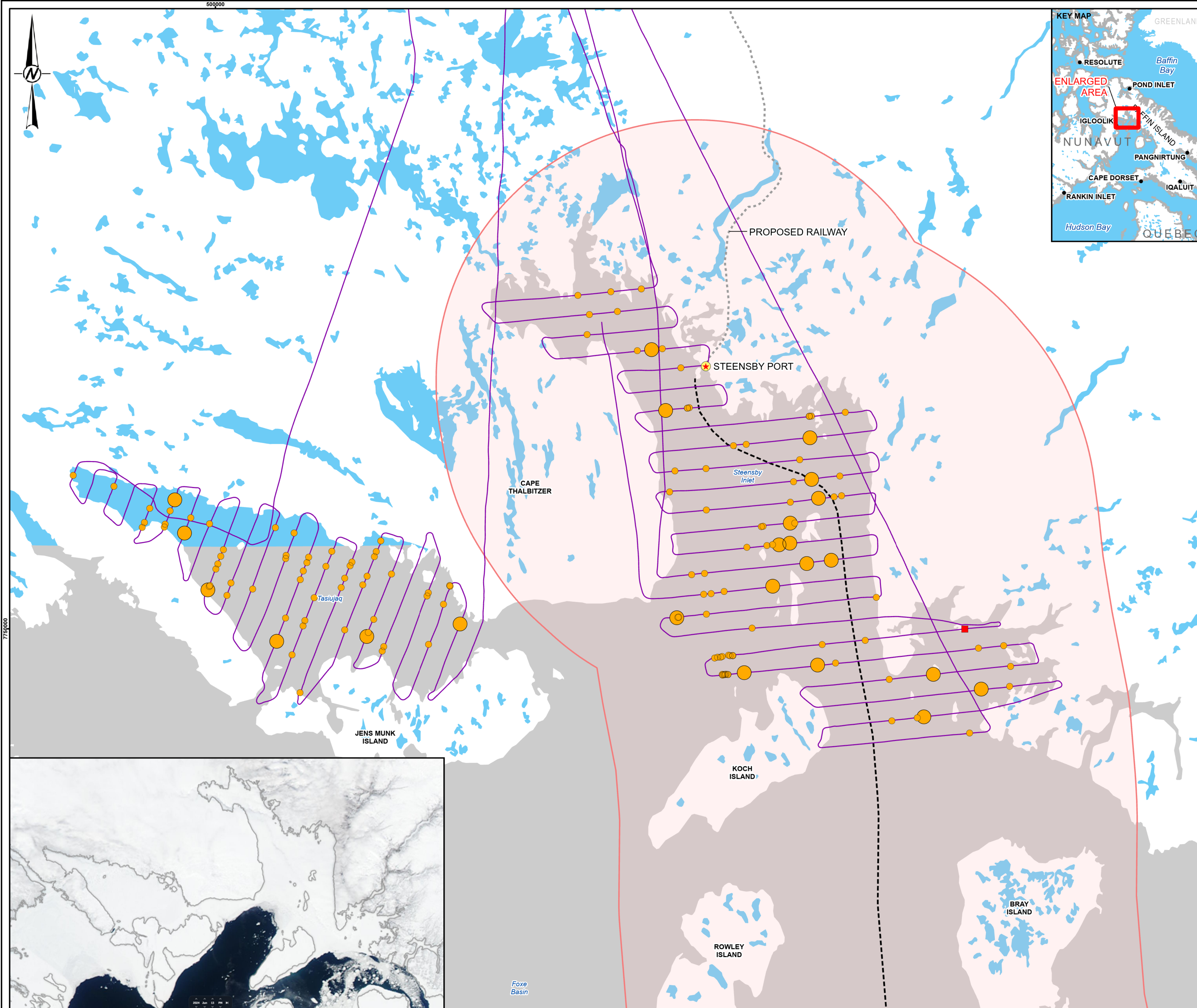

LEGEND

- COMMUNITY
- PORT LOCATION
- PROPOSED RAILWAY
- SHIPPING ROUTE (APPROXIMATE)
- SURVEY TRACK
- LOCAL STUDY AREA
- MARINE REGIONAL STUDY AREA
- WATERBODY

MARINE MAMMAL SPECIES OBSERVATIONS (GROUP SIZE)

POLAR BEAR

- 1

RINGED SEAL

- 1
- 2-4

0 25 50

1:750,000 KILOMETRES

REFERENCE(S)

BASE DATA OBTAINED FROM GEOGRATIS, © DEPARTMENT OF NATURAL RESOURCES CANADA. ALL RIGHTS RESERVED. SHIPPING ROUTE PROVIDED BY CLIENT, JUNE 8, 2022. NUNAVUT SETTLEMENT BOUNDARY OBTAINED FROM NUNAVUT TUNNGAVIK INC., OCTOBER 9, 2012. PROJECTED COORDINATE SYSTEM: NAD 1983 UTM ZONE 17N

CLIENT

BAFFINLAND IRON MINES CORPORATION

PROJECT

MARY RIVER PROJECT
2021 & 2024 RINGED SEAL AERIAL SURVEYS

TITLE

DISTRIBUTION OF RINGED SEALS AND POLAR BEARS RECORDED DURING AERIAL SURVEY ON 9&12 JUNE 2024

CONSULTANT

wsp

YYYY-MM-DD	2025-10-28
DESIGNED	TT
PREPARED	AA
REVIEWED	TT
APPROVED	PA

PROJECT NO.	CONTROL	REV.	FIGURE
CA0051512.6683	1000.01	0	13

3.5 Strip-Transect Density Estimates

Twelve ringed seal observations were excluded from the analysis; nine fell beyond the 125m FLIR transect width, and three were observed during foggy conditions that were excluded from the effort due to reduced visibility. A summary of hauled out ringed seal densities for each survey and strata is presented in Table 2. In 2021, ringed seal densities were 0.948 and 1.188 seals/km² for Steensby and Tasiujaq, respectively, which were higher than those observed in 2024, where densities ranged from 0.476 to 0.742 seals/km². Specifically, in Steensby Inlet, the density estimate in 2021 (0.948 ringed seals/km², CV = 0.125) was statistically significantly greater than the estimates recorded in 2024 (0.476 ringed seals/km², CV = 0.186 and 0.532 ringed seals/km², CV = 0.120) (t-test = 3.19, p = 0.003; t-test = 3.08, p = 0.004, respectively). Likewise, in Tasiujaq, the 2021 density estimate (1.188 ringed seals/km², CV = 0.103) was statistically significantly greater than in 2024 (0.690 ringed seals/km², CV = 0.134 and 0.742 ringed seals/km², CV = 0.134) (t-test = 3.25, p = 0.002; t-test = 2.83, p = 0.007, respectively).

Table 2: Ringed seal density estimates based on aerial surveys flown in 2021 and 2024

Date	Survey #	Stratum	# Observations	# Animals	Density (seal/km^2)	CV	95% CI
13 June 2021	1	Steensby	151	173	0.948	0.125	0.742–1.210
13 June 2021	1	Tasiujaq	106	113	1.188	0.103	0.972–1.453
7–8 June 2024	2	Steensby	79	92	0.476	0.186	0.332–0.683
8 June 2024	2	Tasiujaq	63	67	0.690	0.134	0.531–0.896
9–12 June 2024	3	Steensby	86	105	0.532	0.120	0.420–0.673
12 June 2024	3	Tasiujaq	60	68	0.742	0.134	0.571–0.964
7-12 June 2024	2-3	Steensby	165	197	0.504	0.108	0.408–0.623
8-12 June 2024	2-3	Tasiujaq	123	135	0.715	0.095	0.594–0.861

In 2024, the estimated density of ringed seals for Survey 2 was 0.476 seals/km² (CV = 0.186) in Steensby Inlet and 0.690 seals/km² (CV = 0.134) in Tasiujaq. These values did not differ significantly from those obtained in Survey 3, which recorded densities of 0.532 seals/km² (CV = 0.120) in Steensby Inlet and 0.742 seals/km² (CV = 0.134) in Tasiujaq (t-test = 0.51, p = 0.613; t-test = 0.38, p = 0.703). Accordingly, results from Surveys 2 and 3 were combined to generate mean density estimates of 0.504 seals/km² (CV = 0.108; 95% CI: 0.408–0.623) for Steensby Inlet and 0.715 seals/km² (CV = 0.095; 95% CI: 0.594–0.861) for Tasiujaq (Table 2).

Ringed seal densities exhibited variation between the strata of Steensby Inlet and Tasiujaq. Across all years and surveys, ringed seal densities were consistently 20 to 30% lower in Steensby Inlet than in Tasiujaq; however, these differences were not statistically significant between individual surveys (Survey 1: t-test = 1.41, p = 0.165; Survey 2: t-test = 1.67, p = 0.102; Survey 3: t-test = 1.78, p = 0.084). However, when Surveys 2 and 3 from 2024 were averaged, the difference between the Steensby Inlet and Tasiujaq strata was statistically significant (Survey 2–3: t-test = 2.43 p = 0.017).

3.6 Factors Affecting Proportion of Seals Hauled Out

Univariate analyses were conducted annually employing chi-square (χ^2) goodness-of-fit tests to independently evaluate the associations between observed ringed seals and variables potentially influencing the proportion of seals hauled out. The analysis considered several factors, including time of day, date, air temperature, wind speed, and cloud cover (Table 3).

Table 3: Summary of χ^2 analyses of ringed seal density relative to variables affecting the proportion of seals hauled out.

Variable	Year	Chi-Square	DF	P-value
Time of Day	2021	15.78	7	**0.027**
	2024	7.13	8	0.523
Date	2021	NA	NA	NA
	2024	8.00	3	**0.046**
Air Temperature	2021	9.84	2	**0.007**
	2024	4.92	2	0.085
Wind Speed	2021	17.14	13	0.193
	2024	32.93	15	**0.005**
Cloud Cover	2021	NA	NA	NA
	2024	3.15	6	0.790

Time of Day: Seal density was significantly related to time of day in 2021 in the χ^2 analyses (p=0.027). High seal densities were observed early in the morning at 9:00 and later in the day at 18:00 (Figure 14). In 2024, seal density was not related to time of day in the χ^2 analyses (p=0.523). Seal density increased between 1500 to 1800 in 2021, whereas in 2024 it appeared to decrease between 1300 to 1600. Overall, despite a significant chi-square value in 2021, there seemed to be little pattern in the relationship between seal density and time of day.

Survey Date: Seal density was significantly related to survey date in 2024 in the χ^2 analyses (p=0.046). High seal densities were observed on 12 June compared to lower densities observed during earlier dates of 7–9 June (Figure 14). In 2021, the survey was flown in a single day. As such, no analysis was done for this year.

Air Temperature: In each of the two years, there was a relatively small range in air temperatures. In 2021, seal density was significantly related to air temperatures in the χ^2 analyses (p=0.007), although it was not a linear trend with densities increasing or decreasing with temperature (Figure 14). In 2024, seal density was not related to air temperature in the χ^2 analyses (p=0.085).

Wind Speed: Seal density was significantly related to wind speed in 2024 in the χ^2 analyses (p=0.005). Although 2024 did not show a linear trend with densities increasing or decreasing with wind speed, higher densities were observed at 1 km/h and 11 km/h wind speeds and lower densities were observed at 6 km/h and 17 km/h wind speeds (Figure 14). In 2021, seal density was not related to wind speed in the χ^2 analyses (p=0.193). Despite a significant chi-square value in 2024, effects were inconsistent between the two years.

Cloud Cover: Seal density was not significantly related to cloud cover in 2024 in the χ^2 analyses (p=0.790). In 2021, the survey was flown in only 0% cloud cover. As such, no analysis was done for this year.

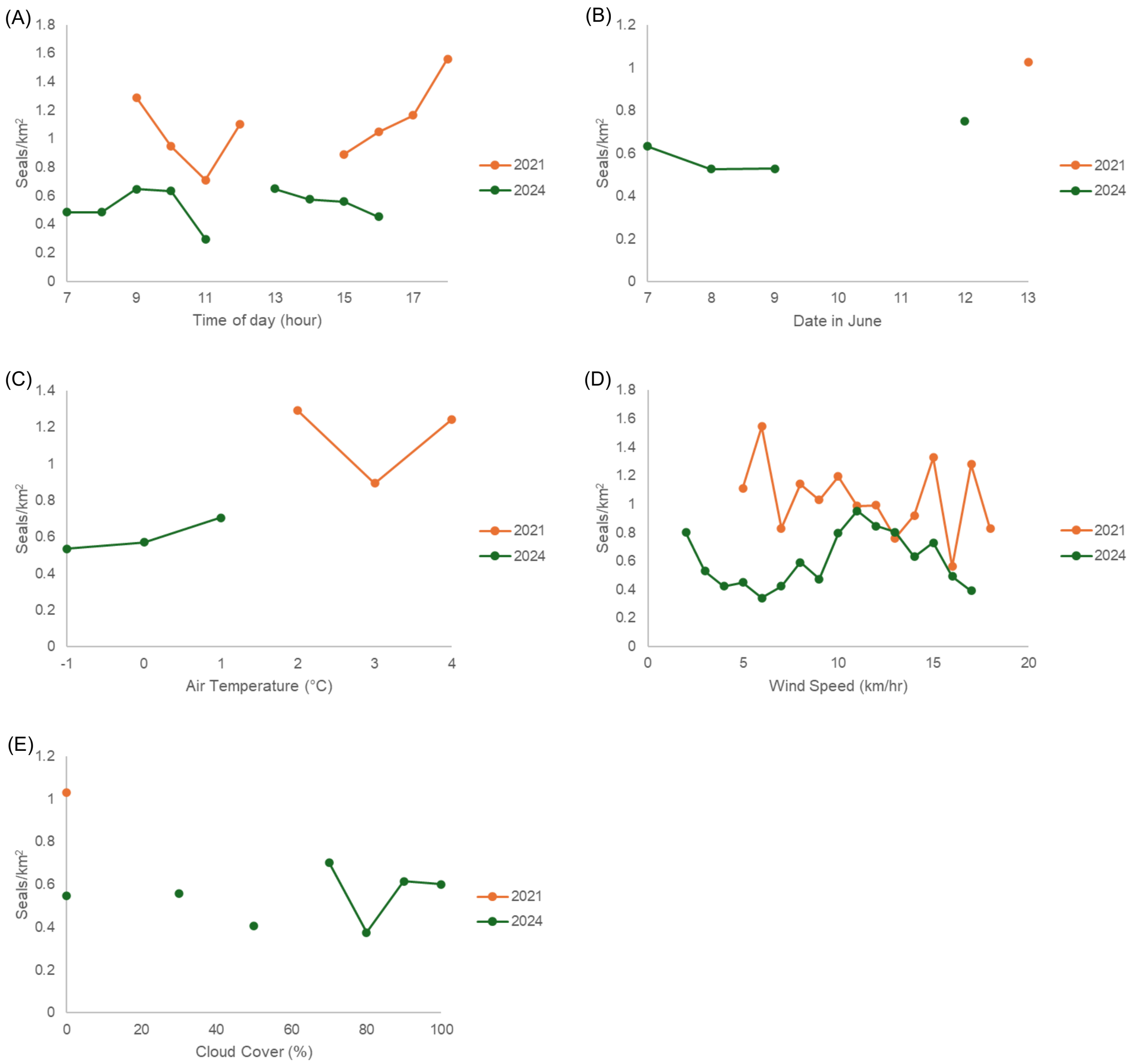

Figure 14: Observed densities of ringed seals during 2021 and 2024 at differing times of day (A), dates (B), values of air temperature (C), wind speed (D), and cloud cover (E).

3.7 Density Surface Modelling

Detection Function Model

A total of 286 and 332 unique ringed seal observations were available for fitting a detection function in 2021 and 2024, respectively.

Since seal sighting counts were expected to dip beneath the aircraft, this would cause a dip in detection at the trackline. Since detection functions are primarily used to model decreasing detections with distance from the trackline, the distances from the trackline were reversed so that what is now zero distance was at the outside edges of the photos and 125 m at the photo center.

Tested models used Uniform, Half-Normal and Hazard Rate detection functions. In this case, the models tested for an animal availability bias rather than observer detection bias. MCDS models were fitted to the data with different key functions, with and without covariates. The model that best fitted the 2021 data was a half-normal key function with one covariate (wind speed) that provided a probability of detection of greater than 98% (p=0.9812). An equivalent model also best fit the 2024 data with a probability of detection of greater than 99.9% (p=0.9999). Since the correction factor due to the detection function was minimal, they were not included in the DSM, with detection assumed to be 100%.

During the 2021 Eclipse Sound survey, the only covariate that proved useful was wind speed, with higher winds resulting in a flatter detection function and lower wind speeds resulting in a greater dip in detections (WSP 2022). Essentially, the noise from the wind appeared to mask the aircraft's approach. For lower wind speeds, it appeared that seals were more likely to dive when the aircraft was directly overhead (a combination of visual and audio cues from the aircraft). Although this relationship was not detected during the Steensby and Tasiujaq surveys, it should be noted that wind speeds were lower during the Eclipse Sound surveys in 2021 (Figure 15), when the effect would be more pronounced.

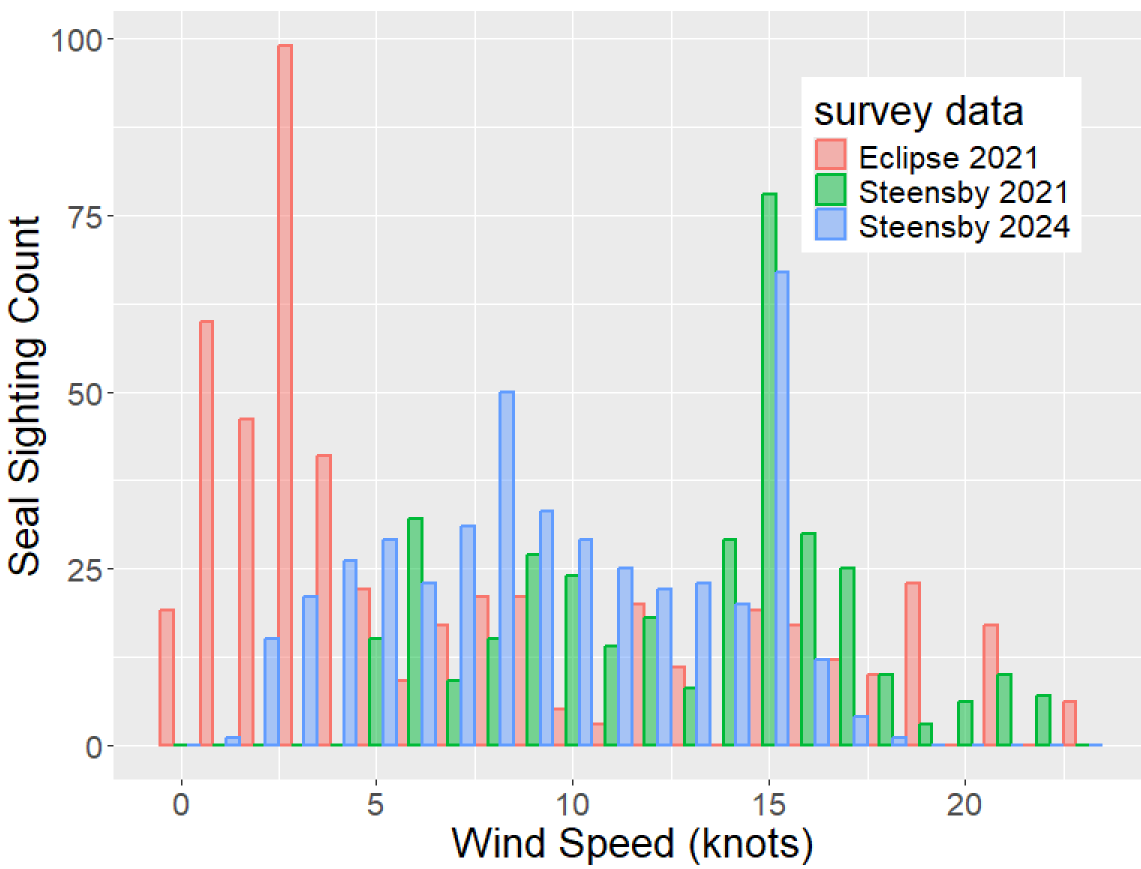

Figure 15: Histogram showing ringed seal observations in relation to wind speeds encountered in the different survey regions and during the different survey years.

Density Surface Models

A table listing the selected DSMs, their associated diagnostic parameters and density estimates are presented in Table 4. The density prediction values for the selected models are presented in Figures 16 through 19, while the spatial representation of the GAM model variance, diagnostic plots, and smooth term plots are presented in Appendix A. Although bivariate spatial smooths were also modeled, all selected models included soap-film spatial smoothers since their results more closely match the survey data.

Density Surface Model – Steensby 2021

The model with a univariate smooth of maximum depth and minimum distance to shore or floe edge, had the lowest AIC of the soap-film spatial smoother models. A visual assessment of this model indicated that the model predictions, as well as the resulting seal density, were more in line with actual observations (0.91 seal/km^2; Figure 16). The p values for the model's spatial smooth was significant ($p < 0.001$), while the primary effects of minimum shore or floe edge distance, and maximum depth were not significant ($p = 0.79$ and 0.44, respectively).

Density Surface Model – Steensby 2024

The model with a univariate smooth of minimum depth and shore distance, had the lowest AIC of the soap-film spatial smoother models. A visual assessment of this model indicated that the model predictions as well as the resulting seal density were more in line with actual observations (0.48 seal/km^2; Figure 17). The p values for the model's spatial smooth was significant ($p < 0.001$), while the primary effects of shore distance, and minimum depth were not significant ($p = 0.41$ and 0.07, respectively).

Density Surface Model – Tasiujaq 2021

The model with a bivariate smooth of minimum depth and shore distance had the lowest AIC of the soap-film spatial smoother models. A visual assessment of this model indicated that the model predictions as well as the resulting seal density were more in line with actual observations (1.20 seal/km^2; Figure 18). The p values for the model's spatial smooth, and interaction between maximum depth and shore distance were significant ($p = 0.01$ and 0.05, respectively) while the primary effects of shore distance and minimum depth on their own, were not significant ($p = 0.98$ and 0.16, respectively).

Density Surface Model – Tasiujaq 2024

The model with a bivariate smooth of minimum depth and shore distance had the lowest AIC of the soap-film spatial smoother models. A visual assessment of this model indicated that the model predictions as well as the resulting seal density were more in line with actual observations (0.71 seal/km^2; Figure 19). The p value for the model's interaction between maximum depth and shore distance was significant ($p = 0.05$) while the spatial smooth, and primary effects of shore distance and minimum depth on their own, were not significant ($p = 0.29$, 0.12 and 0.47, respectively).

The negative binomial distribution family was selected for both of the Steensby models while the Tweedie distribution family was selected for both Tasiujaq models. The selection of the appropriate distribution family was assessed using diagnostic plots (see Appendix A) and the DHARMa function results, and no issues were present for the selected families in the final models. Residual spatial autocorrelation was not found to be significant in any of the selected models, indicating that the model captured the spatial variability in seal counts. The low "deviance explained" values indicate that important covariates are likely missing from the models. Ice type/thickness and tidal currents/heights are likely to be import covariates that could help to explain the distribution of seal sighting but are not available in detail for the study area. The models would likely also benefit from more detailed and accurate bathymetry data if/when available. Details of the selected models are discussed below.

Table 4: Spatial density models for the negative binomial distribution

Year	Strata	GAM Model[a] and distribution family	Covariate edf (# interior knots)	Deviance Explained	Average Density dsm (#/km^2)
2021	Steensby	so(x,y) + s(minDist) + s(maxD) Negative Binomial	22.48, 1.0, 1.0 (131)	16.1%	0.91
2024	Steensby	so(x,y) + s(ShrDst) + s(minD) Negative Binomial	18.6, 1.0, 3.7 (60)	12.7%	0.48
2021	Tasiujaq	so(x,y) + te(ShrDst, minD) + s(minD) + s(ShrDst) Tweedie	18.9, 1.0, 1.0, 1.0 (86)	16.7%	1.20
2024	Tasiujaq	so(x,y) + te(ShrDst, minD) + s(minD) + s(ShrDst) Tweedie	19.4, 1.0, 1.0, 2.7 (86)	11.5%	0.71

[a] "s" = uni variate smooth, "so" = soap-film spatial smooth, "te" = bivariate tensor smooth (does not include primary affect of variables unless stated separately). "minDist" = minimum distance to shore or floe edge, "maxD" = maximum depth, "minD" = minimum depth, "ShrDst" = distance to shore.